Title	Frequency-dependent impedance of a strip foundation group and its representation in time domain
Author(s)	Wang, J; Lo, SH; Zhou, D; Xu, B
Citation	Applied Mathematical Modelling, 2015, v. 39 n. 10-11, p. 2861-2881
Issued Date	2015
URL	http://hdl.handle.net/10722/250261
Rights	This work is licensed under a Creative Commons Attribution-NonCommercial-NoDerivatives 4.0 International License.

Frequency-dependent Impedance of a Strip Foundation Group and its Representation in Time Domain

Jue Wang [a], S. H. Lo [b], Ding Zhou [a,*] Bo-Qing Xu [b]

[a] *College of Civil Engineering, Nanjing University of Technology, Nanjing, China*

[b] *Department of Civil Engineering, the University of Hong Kong, Hong Kong, China*

ABSTRACT

A semi-analytical procedure is presented to study the dynamic cross-interference among a group of long strip foundations on an elastic half space, which is simplified as a two-dimensional problem. In addition to analytical solutions in terms of Green functions, a discretization method is applied to determine the lateral/rocking dynamic impedances of a foundation group. To determine the unknown contact stresses between the foundations and the supporting medium, the soil-foundation interfaces are discretized into a series of strip elements which are only subject to constant lateral and vertical tractions. Multiple foundations with different width and separation distance are considered in the formulations. For the time history analysis of those strongly frequency-dependent impedances of a foundation group through a substructure approach, complex Chebyshev polynomials are used to fit the lumped-parameter (L-P) model in the domain-transformation. Numerical results over a wide range of vibration frequencies for impedance calculation are verified with existing methods. The effects of cross-interference on contact stress distributions and impedances for a group of two and three rigid foundations are discussed in detail. Finally, the accuracy and the validity of the L-P model are rigorously studied by simulating adjacent foundations on an elastic half-space within a close distance.

KEY WORDS: dynamic cross-interference; dynamic impedance; strip foundation group, Green function; lumped-parameter model; complex Chebyshev polynomial

[*] Corresponding author. Tel.: +86 25 58139863.

E-mail address: dingzhou57@yahoo.com (Ding Zhou)

Notations

a_0 = Dimensionless frequency of the excitation

a_m, b_m = Coefficient of the m-th order of the polynomial fraction

G_s = Shear modulus of soil

H_n = Lateral displacement of the n-th foundation

k^∞, c^∞ = Stiffness and damping coefficient at the high-frequency limit

K^s = Static stiffness of foundation

L_n = Width of the n-th foundation in the group

M = Degree of the polynomial

M_n = Amplitude of the rocking excitation on the n-th foundation

N = Number of the surface strip foundations in the group

p_n^r = Uniform vertical traction applied on the r-th element beneath the n-th foundation

q_n^r = Uniform lateral traction applied on the r-th element beneath the n-th foundation

Q_n = Amplitude of the lateral excitation on the n-th foundation

R_n = Elements number of interface beneath n-th foundation

S_n = Separation distance between the n-th foundation and the n-1-th foundation

t_m, t_m^* = The real and complex roots of the denominator of the polynomial

$\tilde{T}_m(\tilde{x})$ = The m-th complex Chebyshev polynomial

${}^pU_n^r(x,z)$ = Lateral displacement field caused by the uniform vertical traction p_n^r

${}^qU_n^r(x,z)$ = Lateral displacement field caused by the uniform lateral traction q_n^r

V_p = Dilatational wave velocity of soil

V_s = Shear wave velocity of soil

${}^pW_n^r(x,z)$ = Vertical displacement field caused by the uniform vertical traction p_n^r

${}^qW_n^r(x,z)$ = Vertical displacement field caused by the uniform lateral traction q_n^r

X, **Y** = Transformation matrices

X_m, X_m^* = The real and complex residues at the pole of polynomial of impedance

Y = Number of complex conjugate pole pairs

Θ_n = Rocking angle of the *n*-th foundation

ξ = Wave number

ρ_s = Mass density of soil

$[\mathfrak{R}]$ = Impedance matrix of the foundation group

$\mathfrak{R}_{mn}^{hh}$ = Lateral impedance between *n*-th foundation and *m*-th foundation

$\mathfrak{R}_{mn}^{rr}$ = Rocking impedance between *n*-th foundation and *m*-th foundation

$\mathfrak{R}_{mn}^{hr}$ (or $\mathfrak{R}_{mn}^{rh}$) = Coupling lateral-rocking impedance between *n*-th foundation and *m*-th foundation

γ_m, μ_m = Coefficients for *m*-th complex Chebyshev polynomial of denominator and numerator

λ_s = Elastic Lamé constant

$\Delta_n = L_n/R_n$ Width of the discretized element for the *n*-th foundation

1. Introduction

Soil-structure interaction (SSI) problem has aroused much interest in research. Various kinds of methods and outcomes have been reported in the past decades [1]. The substructure method, which enables soil and structure to be considered separately, is widely applied in the SSI. In practical situations, structures are sometimes placed close to each other due to a limitation of space. Hence, in the realistic evaluation of their dynamic characteristics, it is necessary to consider not only the interaction between the foundation and the soil medium but also the interaction between foundations through the soil, which is known as structure-soil-structure interaction (SSSI). Besides experimental investigations [2, 3] and numerical procedures [4-6], substructure method is still a powerful and feasible approach to SSSI problems. The two main issues need to be addressed: firstly, how to determine impedance, which is defined as the ratio of a harmonic force applied on the foundation-soil interface to the corresponding harmonic displacement for a group of strip foundations? Secondly, how to incorporate these frequency-dependent impedances to the substructure method for the linear/nonlinear time history analysis?

The analytical solutions for foundation impedance are obtained through a stress boundary-value method, which is based on assumptions [7-9] about the stress distributions (static rigidity, uniform, parabolic or their combinations) underneath the foundation. However, as the assumed distribution may not satisfy the conditions of contact at the foundation-soil interface, the deflected shape of the interface has to be modified based on some averaging techniques. More rigorous solutions for the impedance of foundation can be obtained as a mixed boundary-value problem [10-13] formulated in terms of dual integral equations. Apart from a single strip foundation, those assumed symmetrical distribution of contact stress may not be valid for adjacent or group foundations. On the other hand, as the solutions of dual integral equations cannot be expressed by elementary functions, there are limitations to obtain the contact force functions for a SSSI problem. An approximate method based on the relaxed contact assumption was provided by Warburton et al. [14] to study the dynamic response of two rigid circular foundations on soil medium. The semi-analytical approaches with enhanced flexibility have been widely used to SSSI problems [15-20] . Wong and Luco [21] obtained the dynamic response of a system of rigid surface foundations in frequency domain by the extended

boundary integral method. Savidis and Richter [22] investigated the vertical cross-interference between two rigid, massless, smooth contacting surface foundations by boundary integral equations in conjunction with constant elements in soil-foundation interface. Wang and Schmid [23] studied a similar problem with the full-space Green function. Though the full-space Green function is much simpler than the half-space one [24, 25], the free soil surface around the foundations have to be discretized in addition to foundation-soil interface. Dynamic interaction of arbitrary number of flexible strip foundations resting on smooth contact with a homogeneous elastic half-space was studied by Wang *et al*. [26] based on a classical Green function for a concentrated vertical line load. It was extended later by Senjuntichai and Kaewjuea [27] to a multilayered poroelastic half-space. Their studies were limited to vertical dynamic interaction. However, the lateral/rocking dynamic holds great significance for earthquake engineering as the largest effects of earthquake are on horizontal ground motion rather than vertical ground motion.

Soil-structure interaction analysis by the substructure method is usually applied to the frequency domain because of the frequency-dependent characteristics. The time history response of the superstructure can be obtained by using the fast Fourier transformation (FFT). Since the nonlinear analysis cannot be made in the frequency domain, it is necessary to develop a system with frequency-independent parameters to represent the half-space soil medium so that a nonlinear analysis of the superstructure in the time domain becomes possible. Voigt model can easily and accurately transform the impedance to time domain if the frequency-dependency of the dynamic characteristics is weak. However, the actual impedances usually show strong frequency-dependency due to the SSSI effect or the inhomogeneity of soil [28, 29]. The lumped-parameter (L-P) models, which generally consist of several mechanical components (springs, dashpots, masses and so on.) [30-33], is an effective means to simulate the frequency-dependent characteristics of impedance function in time domain. The coefficients of the mechanical components are determined by the curve-fitting technique or minimizing the discrepancy between the impedance function from the L-P model and that from the rigorous theory. The advantage of the L-P model is that it makes the foundation impedance easily incorporate into an existed time history analysis program even for the nonlinear response of the superstructures. A series of L-P models were presented by Wolf [31-33] to

simulate the impedance of various types of foundations in the time domain. To develop the accuracies of the L-P models, Wolf suggested that the objective functions of the L-P model need to be adapted to make the weight for the low frequencies higher than that of the high frequencies. However, the relation between the frequency and the weight was not clearly clarified. Safak [34] used the *z*-transform together with a Gaussian type weighting function to obtain the objective functions. Wu and Lee [35, 36], and Wang *et al.* [37] developed another set of L-P models by fitting the reciprocal of impedances, which can automatically emphasize the low frequency equations without introducing any weights. Andersen [38] increased the degree of the objective functions to ensure the accuracy of the L-P model of a hexagonal footing. Generally, the stronger frequency-dependent of the impedance, the higher filter order needed to guarantee the sufficient accuracy. However, too high order may cause the wiggling of the approximation [32, 34, 38].

In this paper, a discretization method is proposed to evaluate the lateral/rocking impedance of a rigid strip foundation group intimately attached to an elastic half-space. The influences of the cross-interference effect on the contact stress distributions and the impedances for a group of rigid foundations are discussed in detail. Finally, in extending the substructure method to SSSI problems, Chebyshev polynomial [39, 40] is employed in the L-P model to determine the frequency-dependent characteristics of impedance in time domain, as well as to reduce the problem of wiggling of the approximation with polynomials of high degree.

2. General definition of the cross-interference problem

The lateral/rocking oscillation of a group of N strip foundations of infinite length and different width L_n (n=1, …, N) with full contact to the free surface of an elastic half-space and separation distance S_n is considered as shown in Fig. 1. The geometric and physical parameters of the soil and the foundations are only functions of coordinates x and z. Therefore, the problem can be simplified as a generalized plane strain problem. The lateral excitation $Q_n e^{\mathrm{i}\omega t}$ and the rocking excitation $M_n e^{\mathrm{i}\omega t}$ on each foundation are of the same vibration frequency. The force-displacement relationship for the N foundations considering the cross-interference can be expressed in the following form

$$\begin{Bmatrix} Q_1 \\ \vdots \\ Q_n \\ \vdots \\ Q_N \\ M_1 \\ \vdots \\ M_n \\ \vdots \\ M_N \end{Bmatrix} = \left[\begin{array}{cccccccccc} \Re_{11}^{\mathrm{hh}} & \cdots & \Re_{1n}^{\mathrm{hh}} & \cdots & \Re_{1N}^{\mathrm{hh}} & \Re_{11}^{\mathrm{hr}} & \cdots & \Re_{1n}^{\mathrm{hr}} & \cdots & \Re_{1N}^{\mathrm{hr}} \\ \vdots & \ddots & \vdots & \iddots & \vdots & \vdots & \ddots & \vdots & \iddots & \vdots \\ \Re_{m1}^{\mathrm{hh}} & \cdots & \Re_{mn}^{\mathrm{hh}} & \cdots & \Re_{mN}^{\mathrm{hh}} & \Re_{m1}^{\mathrm{hr}} & \cdots & \Re_{mn}^{\mathrm{hr}} & \cdots & \Re_{mN}^{\mathrm{hr}} \\ \vdots & \iddots & \vdots & \ddots & \vdots & \vdots & \iddots & \vdots & \ddots & \vdots \\ \Re_{N1}^{\mathrm{hh}} & \cdots & \Re_{Nn}^{\mathrm{hh}} & \cdots & \Re_{NN}^{\mathrm{hh}} & \Re_{N1}^{\mathrm{hr}} & \cdots & \Re_{Nn}^{\mathrm{hr}} & \cdots & \Re_{NN}^{\mathrm{hr}} \\ \hdashline \Re_{11}^{\mathrm{rh}} & \cdots & \Re_{1n}^{\mathrm{rh}} & \cdots & \Re_{1N}^{\mathrm{rh}} & \Re_{11}^{\mathrm{rr}} & \cdots & \Re_{1n}^{\mathrm{rr}} & \cdots & \Re_{1N}^{\mathrm{rr}} \\ \vdots & \ddots & \vdots & \iddots & \vdots & \vdots & \ddots & \vdots & \iddots & \vdots \\ \Re_{m1}^{\mathrm{rh}} & \cdots & \Re_{mn}^{\mathrm{rh}} & \cdots & \Re_{mN}^{\mathrm{rh}} & \Re_{m1}^{\mathrm{rr}} & \cdots & \Re_{mn}^{\mathrm{rr}} & \cdots & \Re_{mN}^{\mathrm{rr}} \\ \vdots & \iddots & \vdots & \ddots & \vdots & \vdots & \iddots & \vdots & \ddots & \vdots \\ \Re_{N1}^{\mathrm{hh}} & \cdots & \Re_{Nn}^{\mathrm{rh}} & \cdots & \Re_{NN}^{\mathrm{rh}} & \Re_{N1}^{\mathrm{rr}} & \cdots & \Re_{Nn}^{\mathrm{rr}} & \cdots & \Re_{NN}^{\mathrm{rr}} \end{array}\right] \begin{Bmatrix} H_1 \\ \vdots \\ H_n \\ \vdots \\ H_N \\ \Theta_1 \\ \vdots \\ \Theta_n \\ \vdots \\ \Theta_N \end{Bmatrix} \tag{1}$$

where H_n and Θ_n are the lateral displacement and rocking angle of the n-th foundation, $\Re_{mn}^{\mathrm{hh}}$, $\Re_{mn}^{\mathrm{rr}}$ and $\Re_{mn}^{\mathrm{hr}}$ (or $\Re_{mn}^{\mathrm{rh}}$) are the lateral impedance, rocking impedance and coupling lateral-rocking impedance between n-th foundation and m-th foundation, respectively.

Rewriting Eq. (1) in a more compact form, we have

$$\begin{Bmatrix} \hat{\boldsymbol{Q}} \\ \hat{\boldsymbol{M}} \end{Bmatrix} = [\mathfrak{R}] \begin{Bmatrix} \hat{\boldsymbol{H}} \\ \hat{\boldsymbol{\Theta}} \end{Bmatrix} \tag{2}$$

The impedance matrix [$\mathfrak{R}$] of the system should be determined with due regard for the contact stress distributions of the foundation-soil interfaces. The interface between the soil and each foundation is discretized into a number of surface elements. The elements beneath the n-th foundation (n=1，⋯，N) are numbered sequentially from 1 to R_n, starting from the left to the right. The width of the element is denoted by $\Delta_n=L_n/R_n$ where L_n and R_n are representing the width and the number of divisions for foundation of strip n. The coordinates information for the elements in the system are summarized in Table 1. It is assumed that the r-th element (r=1，⋯，R_n) beneath the n-th foundation is subjected to a uniform lateral traction q_n^r and a vertical traction p_n^r.

3. The half-space Green functions

Based on the Cartesian coordinate system (x-z) with z=0 at the free surface, the wave equations in an elastic half-space of homogeneous solid are given by

$$\begin{cases} (\lambda_s + G_s)\left(\dfrac{\partial^2 u(x,y,t)}{\partial x^2} + \dfrac{\partial^2 w(x,z,t)}{\partial x \partial z}\right) + G_s \nabla^2 u(x,z,t) = \rho_s \dfrac{\partial^2 u(x,z,t)}{\partial t^2} \\ (\lambda_s + G_s)\left(\dfrac{\partial^2 u(x,y,t)}{\partial x \partial z} + \dfrac{\partial^2 w(x,z,t)}{\partial z^2}\right) + G_s \nabla^2 w(x,z,t) = \rho_s \dfrac{\partial^2 w(x,z,t)}{\partial t^2} \end{cases} \tag{3}$$

where ρ_s is the density of the soil, G_s and λ_s are the Lamé constants, u, w are the displacement components in x and z directions. As the foundations are excited by harmonic forces, their steady-state vibrations satisfy $u(x, z, t)=U(x, z)e^{i\omega t}$, $w(x, z, t)=W(x, z)e^{i\omega t}$. For brevity, the time dependence $e^{i\omega t}$ is omitted. $\nabla^2 = \left(\dfrac{\partial^2}{\partial x^2} + \dfrac{\partial^2}{\partial z^2}\right)$ denotes the Laplacian operator.

The general solutions of Eq. (3) for a half-space are obtained by the method of separation of variables, as shown below [24]:

$$\begin{cases} U(x,z) = \int_{-\infty}^{\infty} \left(i\xi e^{-\alpha z} A - \beta e^{-\beta z} B\right) e^{i\xi x} d\xi \\ W(x,z) = \int_{-\infty}^{\infty} \left(-\alpha e^{-\alpha z} A - i\xi e^{-\beta z} B\right) e^{i\xi x} d\xi \end{cases} \tag{4}$$

where $\alpha = \sqrt{\xi^2 - \left(\omega / V_p\right)^2}$, $\beta = \sqrt{\xi^2 - \left(\omega / V_s\right)^2}$, ξ is the wave number, V_p is the dilatational wave (P wave) velocity with $V_p = \sqrt{(\lambda_s + 2G_s)/\rho_s}$; V_s is the shear wave (S wave) velocity with $V_s = \sqrt{G_s / \rho_s}$.

Based on the relationships between stresses and displacements of plane problem in elasticity, we have $\sigma_{zz}(x,z) = 2G_s \dfrac{\partial W(x,z)}{\partial z} + \lambda_s \left(\dfrac{\partial U(x,z)}{\partial x} + \dfrac{\partial W(x,z)}{\partial z}\right)$ and $\tau_{zx}(x,z) = G_s \left(\dfrac{\partial U(x,z)}{\partial z} + \dfrac{\partial W(x,z)}{\partial x}\right)$, the general solutions for stresses σ_{zz} and τ_{xz} can be expressed as

$$\begin{cases} \sigma_{zz}(x,z) = G_s \int_{-\infty}^{\infty} \left\{\left[2\xi^2 - \left(\omega / V_s\right)^2\right] e^{-\alpha z} A + i2\xi\beta e^{-\beta z} B\right\} e^{i\xi x} d\xi \\ \tau_{zx}(x,z) = G_s \int_{-\infty}^{\infty} \left\{-i2\xi\alpha e^{-\alpha z} A + \left[2\xi^2 - \left(\omega / V_s\right)^2\right] e^{-\beta z} B\right\} e^{i\xi x} d\xi \end{cases} \tag{5}$$

3.1. Lateral harmonic traction

Without loss of generality, consider the lateral uniform traction q_n^r applied at the interval $[x_{n1}^r, x_{n2}^r]$ as shown in Fig. 2(a). The boundary conditions at ground surface z=0 are given by

$$\sigma_{zz}(x,0)=0\,,\qquad \tau_{xz}(x,0)=\begin{cases}-q_n^r & x_{n1}^r\le x\le x_{n2}^r\\ 0 & \text{others}\end{cases} \tag{6}$$

Based on the Fourier transformation pairs $F(\xi)=\int_{-\infty}^{\infty}f(x)\mathrm{e}^{-\mathrm{i}\xi x}\mathrm{d}x$ and $f(x)=\frac{1}{2\pi}\int_{-\infty}^{\infty}F(\xi)\mathrm{e}^{\mathrm{i}\xi x}\mathrm{d}\xi$, Eq. (6) can be expressed in the integral form:

$$\sigma_{zz}(x,0)=\frac{1}{2\pi}\int_{-\infty}^{\infty}0\;d\xi\,,\qquad \tau_{zx}(x,0)=\mathrm{i}\frac{q_n^r}{2\pi}\int_{-\infty}^{\infty}\frac{1}{\xi}\left[e^{\mathrm{i}\left(x-x_{n1}^r\right)\xi}-e^{\mathrm{i}\left(x-x_{n2}^r\right)\xi}\right]\mathrm{d}\xi \tag{7}$$

Comparing Eq. (7) with Eq. (5), the coefficients *A* and *B* can be determined

$$A=\frac{\beta q_n^r\left(e^{-\mathrm{i}\xi x_{n1}^r}-e^{-\mathrm{i}\xi x_{n2}^r}\right)}{\pi G_s F(\xi)},\qquad B=\mathrm{i}\frac{q_n^r\left[2\xi^2-\left(\omega/V_s\right)^2\right]\left(e^{-\mathrm{i}\xi x_{n1}^r}-e^{-\mathrm{i}\xi x_{n2}^r}\right)}{2\pi G_s\xi F(\xi)} \tag{8}$$

Substituting the above two coefficients back to Eq. (4), the displacements ${}^qU_n^r(x,z)$ and ${}^qW_n^r(x,z)$ due to q_n^r can be expressed as

$${}^qU_n^r(x,z)=\mathrm{i}\frac{q_n^r}{2\pi G_s}\int_{-\infty}^{\infty}\frac{\beta\left[2\xi^2\mathrm{e}^{-\alpha z}-\left(2\xi^2-\left(\omega/V_s\right)^2\right)\mathrm{e}^{-\beta z}\right]}{\xi F(\xi)}\left[e^{\mathrm{i}\xi\left(x-x_{n1}^r\right)}-e^{\mathrm{i}\xi\left(x-x_{n2}^r\right)}\right]d\xi \tag{9}$$

$${}^qW_n^r(x,z)=-\mathrm{i}\frac{q_n^r}{2\pi G_s}\int_{-\infty}^{\infty}\frac{\alpha\left[\left(2\xi^2-\left(\omega/V_s\right)^2\right)\mathrm{e}^{-\alpha z}+2\xi^2\,\mathrm{e}^{-\beta z}\right]}{\xi F(\xi)}\left[e^{\mathrm{i}\xi\left(x-x_{n1}^r\right)}-e^{\mathrm{i}\xi\left(x-x_{n2}^r\right)}\right]d\xi \tag{10}$$

in which, $F(\xi)=\left[2\xi^2-\left(\omega/V_s\right)^2\right]^2-4\xi^2\alpha\beta$.

To transform the results to a more convenient form for calculation, we let $\xi=\eta\omega/V_s$, $\vartheta=V_s/V_p$ and then $F(\xi)$ can be transformed into $F(\eta)=(2\eta^2-1)^2-4\eta^2\sqrt{\eta^2-\vartheta^2}\sqrt{\eta^2-1}$. Substituting the *r*-th element of foundation *n* (shown in Table 1) into Eqs. (9) and (10) and making use of the symmetry of the integral, the lateral and vertical surface displacements of soil due to the lateral traction q_n^r are, respectively, given by

$${}^qU_n^r(x,0)=-\frac{q_n^rV_s}{\pi\omega G_s}\int_0^{\infty}\frac{\sqrt{\eta^2-1}}{\eta F(\eta)}\left\{\sin\frac{\eta\omega}{V_s}\left[x-\frac{(r-1)L_n}{N_n}-\sum_{l=1}^{n}\left(S_l+L_{l-1}\right)\right]-\sin\frac{\eta\omega}{V_s}\left[x-\frac{rL_n}{N_n}-\sum_{l=1}^{n}\left(S_l+L_{l-1}\right)\right]\right\}d\eta \tag{11}$$

$$ {}^{q}W_n^r(x,0)=\frac{q_n^r V_s}{\pi\omega G_s}\int_0^{\infty}\frac{\left(2\eta^2-1-2\sqrt{\eta^2-\vartheta^2}\sqrt{\eta^2-1}\right)}{F(\eta)}\left\{\cos\left[\frac{\eta\omega}{V_s}\left(x-\frac{(r-1)L_n}{N_n}-\sum_{l=1}^{n}\left(S_l+L_{l-1}\right)\right)\right]-\right. $$
$$ \left.\cos\left[\frac{\eta\omega}{V_s}\left(x-\frac{rL_n}{N_n}-\sum_{l=1}^{n}\left(S_l+L_{l-1}\right)\right)\right]\right\}\mathrm{d}\eta \tag{12} $$

3.2. Vertical harmonic traction

Consider the vertical uniform traction p_n^r applied at the interval $[x_{n1}^r, x_{n2}^r]$, as shown in Fig. 2(b). The boundary condition at ground surface z=0 are given by

$$ \sigma_{zz}(x,0)=\begin{cases}-p_n^r & x_{n1}^r\le x\le x_{n2}^r\\ 0 & \text{others}\end{cases},\qquad \tau_{xz}(x,0)=0 \tag{13} $$

Applying Fourier transformation to Eq. (13) and expressing it in integral form, we have

$$ \sigma_{zz}(x,0)=-\frac{p_n^r}{2\pi\mathrm{i}}\int_{-\infty}^{\infty}\frac{1}{\xi}\left[\mathrm{e}^{\mathrm{i}\xi(x-x_{n1}^r)}-e^{\mathrm{i}\xi(x-x_{n2}^r)}\right]\mathrm{d}\xi,\qquad \tau_{xz}(x,0)=\frac{1}{2\pi}\int_{-\infty}^{\infty}0\ \mathrm{d}\xi \tag{14} $$

Comparing Eq. (14) with Eq. (5), the coefficients A and B can be determined

$$ A=\mathrm{i}\frac{p_n^r\left[2\xi^2-\left(\omega/V_s\right)^2\right]\left(e^{-\mathrm{i}\xi x_{n1}^r}-e^{-\mathrm{i}\xi x_{n2}^r}\right)}{2\pi G_s\xi F(\xi)},\qquad B=-\frac{p_n^r\alpha\left(e^{-\mathrm{i}\xi x_{n1}^r}-e^{-\mathrm{i}\xi x_{n2}^r}\right)}{\pi G_s F(\xi)} \tag{15} $$

Substituting coefficients A and B back to Eq. (4), the displacements due to p_n^r are given by

$$ {}^{p}U_n^r(x,z)=-\frac{p_n^r}{2\pi G_s}\int_{-\infty}^{\infty}\frac{\left[2\xi^2-\left(\omega/V_s\right)^2\right]\mathrm{e}^{-\alpha z}-2\alpha\beta e^{-\beta z}}{F(\xi)}\left[e^{\mathrm{i}\xi(x-x_{n1}^r)}-e^{\mathrm{i}\xi(x-x_{n2}^r)}\right]\mathrm{d}\xi \tag{16} $$

$$ {}^{p}W_n^r(x,z)=-\mathrm{i}\frac{p_n^r}{2\pi G_s}\int_{-\infty}^{\infty}\frac{\alpha\left[\left(2\xi^2-\left(\omega/V_s\right)^2\right)\mathrm{e}^{-\alpha z}+2\xi^2 e^{-\beta z}\right]}{\xi F(\xi)}\left[e^{\mathrm{i}\xi(x-x_{n1}^r)}-e^{\mathrm{i}\xi(x-x_{n2}^r)}\right]\mathrm{d}\xi \tag{17} $$

Similar to the transformation given in section 3.1, the lateral and vertical surface displacements of soil due to the vertical traction p_n^r are, respectively, written as

$$ {}^{p}U_n^r(x,0)=-\frac{p_n^r V_s}{\pi\omega G_s}\int_0^{\infty}\frac{\left(2\eta^2-1-2\sqrt{\eta^2-\vartheta^2}\sqrt{\eta^2-1}\right)}{F(\eta)}\left\{\cos\left[\frac{\eta\omega}{V_s}\left(x-\frac{(r-1)L_n}{N_n}-\sum_{l=1}^{n}\left(S_l+L_{l-1}\right)\right)\right]-\right. $$
$$ \left.\cos\left[\frac{\eta\omega}{V_s}\left(x-\frac{rL_n}{N_n}-\sum_{l=1}^{n}\left(S_l+L_{l-1}\right)\right)\right]\right\}\mathrm{d}\eta \tag{18} $$

$$ {}^{p}W_n^r(x,0) = -\frac{p_n^r V_s}{\pi\omega G_s}\int_0^{\infty}\frac{\sqrt{\eta^2-\vartheta^2}}{\eta F(\eta)}\left\{\sin\left[\frac{\eta\omega}{V_s}\left(x-\frac{(r-1)L_n}{N_n}-\sum_{l=1}^{n}\left(S_l+L_{l-1}\right)\right)\right]-\sin\left[\frac{\eta\omega}{V_s}\left(x-\frac{rL_n}{N_n}-\sum_{l=1}^{n}\left(S_l+L_{l-1}\right)\right)\right]\right\}\mathrm{d}\eta \quad (19) $$

4. Evaluation of lateral/rocking impedance for a foundation group

Based on the superposition principle, the lateral displacement $U(x, 0)$ and the vertical displacement $W(x, 0)$ of the soil surface due to a series of tractions q_n^r and p_n^r (n=1,2,...,N) can be obtained from Eqs. (11), (12), (18) and (19):

$$ U(x,0) = \sum_{n=1}^{N}\sum_{r=1}^{R_n} {}^{q}U_n^r(x,0) + \sum_{n=1}^{N}\sum_{r=1}^{R_n} {}^{p}U_n^r(x,0) \quad (20) $$

$$ W(x,0) = \sum_{n=1}^{N}\sum_{r=1}^{R_n} {}^{q}W_n^r(x,0) + \sum_{n=1}^{N}\sum_{r=1}^{R_n} {}^{p}W_n^r(x,0) \quad (21) $$

The total lateral and vertical surface displacements U_n^r and W_n^r of the r-th element beneath the n-th foundation can be obtained by substituting the coordinate of the r-th element to Eq. (20) and Eq. (21), respectively. Consequently, the following flexibility equation of the system can be established as follows

$$ \begin{Bmatrix} \hat{\boldsymbol{U}}_1 \\ \vdots \\ \hat{\boldsymbol{U}}_n \\ \vdots \\ \hat{\boldsymbol{U}}_N \\ \hat{\boldsymbol{W}}_1 \\ \vdots \\ \hat{\boldsymbol{W}}_n \\ \vdots \\ \hat{\boldsymbol{W}}_N \end{Bmatrix} = \left[\begin{array}{cccccc|cccccc} \left[\boldsymbol{A}_{11}^{R_1R_1}\right] & \cdots & \left[\boldsymbol{A}_{1n}^{R_1R_n}\right] & \cdots & \left[\boldsymbol{A}_{1N}^{R_1R_N}\right] & & \left[\boldsymbol{B}_{11}^{R_1R_1}\right] & \cdots & \left[\boldsymbol{B}_{1n}^{R_1R_n}\right] & \cdots & \left[\boldsymbol{B}_{1N}^{R_1R_N}\right] \\ \vdots & \ddots & \vdots & \iddots & \vdots & & \vdots & \ddots & \vdots & \iddots & \vdots \\ \left[\boldsymbol{A}_{m2}^{R_mR_2}\right] & \cdots & \left[\boldsymbol{A}_{mn}^{R_mR_n}\right] & \cdots & \left[\boldsymbol{A}_{mN}^{R_mR_N}\right] & & \left[\boldsymbol{B}_{m2}^{R_mR_2}\right] & \cdots & \left[\boldsymbol{B}_{mn}^{R_mR_n}\right] & \cdots & \left[\boldsymbol{B}_{mN}^{R_mR_N}\right] \\ \vdots & \iddots & \vdots & \ddots & \vdots & & \vdots & \iddots & \vdots & \ddots & \vdots \\ \left[\boldsymbol{A}_{N1}^{R_NR_1}\right] & \cdots & \left[\boldsymbol{A}_{Nn}^{R_NR_n}\right] & \cdots & \left[\boldsymbol{A}_{NN}^{R_NR_N}\right] & & \left[\boldsymbol{B}_{N1}^{R_NR_1}\right] & \cdots & \left[\boldsymbol{B}_{Nn}^{R_NR_n}\right] & \cdots & \left[\boldsymbol{B}_{NN}^{R_NR_N}\right] \\ \hline \left[\boldsymbol{C}_{11}^{R_1R_1}\right] & \cdots & \left[\boldsymbol{C}_{1n}^{R_1R_n}\right] & \cdots & \left[\boldsymbol{C}_{1N}^{R_1R_N}\right] & & \left[\boldsymbol{D}_{11}^{R_1R_1}\right] & \cdots & \left[\boldsymbol{D}_{1n}^{R_1R_n}\right] & \cdots & \left[\boldsymbol{D}_{1N}^{R_1R_N}\right] \\ \vdots & \ddots & \vdots & \iddots & \vdots & & \vdots & \ddots & \vdots & \iddots & \vdots \\ \left[\boldsymbol{C}_{m2}^{R_mR_2}\right] & \cdots & \left[\boldsymbol{C}_{mn}^{R_mR_n}\right] & \cdots & \left[\boldsymbol{C}_{mN}^{R_mR_N}\right] & & \left[\boldsymbol{D}_{m2}^{R_mR_2}\right] & \cdots & \left[\boldsymbol{D}_{mn}^{R_mR_n}\right] & \cdots & \left[\boldsymbol{D}_{mN}^{R_mR_N}\right] \\ \vdots & \iddots & \vdots & \ddots & \vdots & & \vdots & \iddots & \vdots & \ddots & \vdots \\ \left[\boldsymbol{C}_{N1}^{R_NR_1}\right] & \cdots & \left[\boldsymbol{C}_{Nn}^{R_NR_n}\right] & \cdots & \left[\boldsymbol{C}_{NN}^{R_NR_N}\right] & & \left[\boldsymbol{D}_{N1}^{R_NR_1}\right] & \cdots & \left[\boldsymbol{D}_{Nn}^{R_NR_n}\right] & \cdots & \left[\boldsymbol{D}_{NN}^{R_NR_N}\right] \end{array}\right] \begin{Bmatrix} \hat{\boldsymbol{q}}_1 \\ \vdots \\ \hat{\boldsymbol{q}}_n \\ \vdots \\ \hat{\boldsymbol{q}}_N \\ \hat{\boldsymbol{p}}_1 \\ \vdots \\ \hat{\boldsymbol{p}}_n \\ \vdots \\ \hat{\boldsymbol{p}}_N \end{Bmatrix} \quad (22) $$

in which, $\hat{\boldsymbol{q}}_n = \left\{q_n^1,\ q_n^2,\ \cdots,\ q_n^{R_n}\right\}^T$; $\hat{\boldsymbol{p}}_n = \left\{p_n^1,\ p_n^2,\ \cdots,\ p_n^{R_n}\right\}^T$; $\hat{\boldsymbol{U}}_n = \left\{U_n^1,\ U_n^2,\ \cdots,\ U_n^{R_n}\right\}^T$;

$\hat{\boldsymbol{W}}_n = \left\{W_n^1,\ W_n^2,\ \cdots,\ W_n^{R_n}\right\}^T$. And

$$\left[\boldsymbol{A}_{mn}^{R_m R_n}\right]=\begin{bmatrix} \overline{A}_{mn}^{11} & \cdots & \overline{A}_{mn}^{1j} & \cdots & \overline{A}_{mn}^{1R_n} \\ \vdots & \ddots & \vdots & \iddots & \vdots \\ \overline{A}_{mn}^{i1} & \cdots & \overline{A}_{mn}^{ij} & \cdots & \overline{A}_{mn}^{iR_n} \\ \vdots & \iddots & \vdots & \ddots & \vdots \\ \overline{A}_{mn}^{R_m 1} & \cdots & \overline{A}_{mn}^{R_m j} & \cdots & \overline{A}_{mn}^{R_m R_n} \end{bmatrix}, n, m=1, 2, \ldots, N; i=1, 2, \ldots, R_m; j=1, 2, \ldots, R_n \tag{23}$$

in which, element $\overline{A}_{mn}^{ij}$ describes the relationship between the lateral traction q_n^j applied on the j-th element of the n-th foundation and the lateral displacement U_m^i for the i-th element of the the m-th foundation.

$$\overline{A}_{mn}^{ij}=-\frac{V_s}{\pi\omega G_s}\int_0^{\infty}\frac{\sqrt{\eta^2-1}}{\eta F(\eta)}G_1(m,n,i,j,\eta)d\eta \tag{24}$$

where

$$G_1(m,n,i,j,\eta)=\sin\left[\eta\frac{\omega}{V_s}\left(\frac{(2i-1)L_m}{2R_m}+\sum_{l=1}^{m}(S_l+L_{l-1})-\left(\frac{(j-1)L_n}{R_n}+\sum_{l=1}^{n}(S_l+L_{l-1})\right)\right)\right]- \sin\left[\eta\frac{\omega}{V_s}\left(\frac{(2i-1)L_m}{2R_m}+\sum_{l=1}^{m}(S_l+L_{l-1})-\left(\frac{jL_n}{R_n}+\sum_{l=1}^{n}(S_l+L_{l-1})\right)\right)\right] \tag{25}$$

$$\left[\boldsymbol{B}_{mn}^{R_m R_n}\right]=\begin{bmatrix} \overline{B}_{mn}^{11} & \cdots & \overline{B}_{mn}^{1j} & \cdots & \overline{B}_{mn}^{1R_n} \\ \vdots & \ddots & \vdots & \iddots & \vdots \\ \overline{B}_{mn}^{i1} & \cdots & \overline{B}_{mn}^{ij} & \cdots & \overline{B}_{mn}^{iR_n} \\ \vdots & \iddots & \vdots & \ddots & \vdots \\ \overline{B}_{mn}^{R_m 1} & \cdots & \overline{B}_{mn}^{R_m j} & \cdots & \overline{B}_{mn}^{R_m R_n} \end{bmatrix} \tag{26}$$

in which, element $\overline{B}_{mn}^{ij}$ in matrix $\left[\boldsymbol{B}_{mn}^{R_m R_n}\right]$ describes the relationship between the vertical traction p_n^j applied on the j-th element of the n-th foundation and the lateral displacement U_m^i for the i-th element of the m-th foundation.

$$\overline{B}_{mn}^{ij}=-\frac{V_s}{\pi\omega G_s}\int_0^{\infty}\frac{2\eta^2-1-2\sqrt{\eta^2-\vartheta^2}\sqrt{\eta^2-1}}{F(\eta)}G_2(m,n,i,j,\eta)\mathrm{d}\eta \tag{27}$$

in which,

$$G_2(m,n,i,j,\eta)=\cos\left[\eta\frac{\omega}{V_s}\left(\frac{(2i-1)L_m}{2R_m}+\sum_{l=1}^{m}(S_l+L_{l-1})-\left(\frac{(j-1)L_n}{R_n}+\sum_{l=1}^{n}(S_l+L_{l-1})\right)\right)\right]-$$

$$\cos\left[\eta\frac{\omega}{V_s}\left(\frac{(2i-1)L_m}{2R_m}+\sum_{l=1}^{m}(S_l+L_{l-1})-\left(\frac{jL_n}{R_n}+\sum_{l=1}^{n}(S_l+L_{l-1})\right)\right)\right] \tag{28}$$

$$\left[\boldsymbol{C}_{mn}^{R_mR_n}\right]=\begin{bmatrix}\overline{C}_{mn}^{11} & \cdots & \overline{C}_{mn}^{1j} & \cdots & \overline{C}_{mn}^{1R_n}\\ \vdots & \ddots & \vdots & \iddots & \vdots\\ \overline{C}_{mn}^{i1} & \cdots & \overline{C}_{mn}^{ij} & \cdots & \overline{C}_{mn}^{iR_n}\\ \vdots & \iddots & \vdots & \ddots & \vdots\\ \overline{C}_{mn}^{R_m1} & \cdots & \overline{C}_{mn}^{R_mj} & \cdots & \overline{C}_{mn}^{R_mR_n}\end{bmatrix} \tag{29}$$

in which, element $\overline{C}_{mn}^{ij}$ in matrix $\left[\boldsymbol{C}_{mn}^{R_mR_n}\right]$ describes the relationship between the lateral traction q_n^j applied on the *j*-th element of the *n*-th foundation and the vertical displacement W_m^i for the *i*-th element ofthe *m*-th foundation.

$$\overline{C}_{mn}^{ij}=\frac{V_s}{\pi\omega G_s}\int_0^{\infty}\frac{2\eta^2-1-2\sqrt{\eta^2-\vartheta^2}\sqrt{\eta^2-1}}{F(\eta)}G_2(m,n,i,j,\eta)\mathrm{d}\eta \tag{30}$$

Comparing Eq. (27) and Eq. (30), it can be found that $\overline{C}_{mn}^{ij}=-\overline{B}_{mn}^{ij}$.

$$\left[\boldsymbol{D}_{mn}^{R_mR_n}\right]=\begin{bmatrix}\overline{D}_{mn}^{11} & \cdots & \overline{D}_{mn}^{1j} & \cdots & \overline{D}_{mn}^{1R_n}\\ \vdots & \ddots & \vdots & \iddots & \vdots\\ \overline{D}_{mn}^{i1} & \cdots & \overline{D}_{mn}^{ij} & \cdots & \overline{D}_{mn}^{iR_n}\\ \vdots & \iddots & \vdots & \ddots & \vdots\\ \overline{D}_{mn}^{R_m1} & \cdots & \overline{D}_{mn}^{R_mj} & \cdots & \overline{D}_{mn}^{R_mR_n}\end{bmatrix} \tag{31}$$

in which, element $\overline{D}_{mn}^{ij}$ in matrix $\left[\boldsymbol{D}_{mn}^{R_mR_n}\right]$ describes the relationship between the vertical traction p_n^j applied on the *j*-th element of the *n*-th foundation and the vertical displacement W_m^i for the *i*-th element of the *m*-th foundation.

$$\overline{D}_{mn}^{ij}=-\frac{V_s}{\pi\omega G_s}\int_0^{\infty}\frac{\sqrt{\eta^2-\vartheta^2}}{\eta F(\eta)}G_1(m,n,i,j,\eta)d\eta \tag{32}$$

$\overline{A}_{mn}^{ij}$, $\overline{B}_{mn}^{ij}$, $\overline{C}_{mn}^{ij}$ and $\overline{D}_{mn}^{ij}$ are all the multi-value improper integrals, which can be evaluated by using the piecewise integration method, as shown in Appendix.

For brevity, Eq. (22) is rewritten as

$$\begin{bmatrix} \boldsymbol{A} & \boldsymbol{B} \\ \boldsymbol{C} & \boldsymbol{D} \end{bmatrix} \begin{Bmatrix} \hat{\boldsymbol{q}} \\ \hat{\boldsymbol{p}} \end{Bmatrix} = \begin{Bmatrix} \hat{\boldsymbol{U}} \\ \hat{\boldsymbol{W}} \end{Bmatrix} \tag{33}$$

In consideration of the full contact between the rigid foundations and the soil, the displacement of the surface soil elements beneath the *n*-th rigid foundation, we have $\hat{\boldsymbol{U}}_n = H_n \hat{\boldsymbol{I}}_n$ and $\hat{\boldsymbol{W}}_n = \Theta_n \hat{\boldsymbol{E}}_n$, in which $\hat{\boldsymbol{I}}_n$ is a unit column vector of order R_n such that $\hat{\boldsymbol{I}}_n = \{\underbrace{1, \cdots, 1}_{R_n}\}^T$ and $\hat{\boldsymbol{E}}_n$ is a column vector of order R_n such that $\hat{\boldsymbol{E}}_n = \left\{ \frac{(1-R_n)L_n}{2R_n}, \cdots, \frac{(2r-1-R_n)L_n}{2R_n}, \cdots, \frac{(R_n-1)L_n}{2R_n} \right\}^T$. Considering the system shown in Fig. 1, the relationship between displacements of all the surface soil elements and those of the footing group, we have

$$\begin{Bmatrix} \hat{\boldsymbol{U}} \\ \hat{\boldsymbol{W}} \end{Bmatrix} = \begin{bmatrix} \boldsymbol{X} & \boldsymbol{0} \\ \boldsymbol{0} & \boldsymbol{Y} \end{bmatrix} \begin{Bmatrix} \hat{\boldsymbol{H}} \\ \hat{\Theta} \end{Bmatrix} \tag{34}$$

where $\boldsymbol{X}$ and $\boldsymbol{Y}$ are both transformation matrices of dimension $\left(\sum_{n=1}^{N} R_n \right) \times N$,

$$\boldsymbol{X} = \begin{bmatrix} \hat{\boldsymbol{I}}_1 & \hat{\boldsymbol{0}} & \cdots & \hat{\boldsymbol{0}} & \cdots & \hat{\boldsymbol{0}} \\ \hat{\boldsymbol{0}} & \hat{\boldsymbol{I}}_2 & \cdots & \hat{\boldsymbol{0}} & \cdots & \hat{\boldsymbol{0}} \\ \vdots & \vdots & \ddots & \vdots & \ddots & \vdots \\ \hat{\boldsymbol{0}} & \hat{\boldsymbol{0}} & \cdots & \hat{\boldsymbol{I}}_n & \cdots & \hat{\boldsymbol{0}} \\ \vdots & \vdots & \ddots & \vdots & \ddots & \vdots \\ \hat{\boldsymbol{0}} & \hat{\boldsymbol{0}} & \cdots & \hat{\boldsymbol{0}} & \cdots & \hat{\boldsymbol{I}}_N \end{bmatrix}; \quad \boldsymbol{Y} = \begin{bmatrix} \hat{\boldsymbol{E}}_1 & \hat{\boldsymbol{0}} & \cdots & \hat{\boldsymbol{0}} & \cdots & \hat{\boldsymbol{0}} \\ \hat{\boldsymbol{0}} & \hat{\boldsymbol{E}}_2 & \cdots & \hat{\boldsymbol{0}} & \cdots & \hat{\boldsymbol{0}} \\ \vdots & \vdots & \ddots & \vdots & \ddots & \vdots \\ \hat{\boldsymbol{0}} & \hat{\boldsymbol{0}} & \cdots & \hat{\boldsymbol{E}}_n & \cdots & \hat{\boldsymbol{0}} \\ \vdots & \vdots & \ddots & \vdots & \ddots & \vdots \\ \hat{\boldsymbol{0}} & \hat{\boldsymbol{0}} & \cdots & \hat{\boldsymbol{0}} & \cdots & \hat{\boldsymbol{E}}_N \end{bmatrix} \tag{35}$$

Equating the excitation and the contact tractions for the *n*-th foundation yields $Q_n = \Delta_n \sum_{r=1}^{R_n} q_n^r$, $M_n = \sum_{r=1}^{R_n} p_n^r \Delta_n \frac{(2r-R_n)L_n}{2R_n}$. For the entire foundation group we have

$$\begin{Bmatrix} \hat{\boldsymbol{Q}} \\ \hat{\boldsymbol{M}} \end{Bmatrix} = \begin{bmatrix} \Delta \boldsymbol{X} & \boldsymbol{0} \\ \boldsymbol{0} & \Delta \boldsymbol{Y} \end{bmatrix}^T \begin{Bmatrix} \hat{\boldsymbol{q}} \\ \hat{\boldsymbol{p}} \end{Bmatrix} \tag{36}$$

with $\Delta = \text{diag}\left\{ \Delta_1 \left(\hat{\boldsymbol{I}}_1 \right)^T, \cdots, \Delta_N \left(\hat{\boldsymbol{I}}_N \right)^T \right\}$.

Substituting Eqs. (33) and (34) into Eq. (36) leads to

$$\begin{Bmatrix} \hat{\boldsymbol{Q}} \\ \hat{\boldsymbol{M}} \end{Bmatrix} = \begin{bmatrix} \Delta \boldsymbol{X} & \boldsymbol{0} \\ \boldsymbol{0} & \Delta \boldsymbol{Y} \end{bmatrix}^T \begin{bmatrix} \boldsymbol{A} & \boldsymbol{B} \\ \boldsymbol{C} & \boldsymbol{D} \end{bmatrix}^T \begin{bmatrix} \boldsymbol{X} & \boldsymbol{0} \\ \boldsymbol{0} & \boldsymbol{Y} \end{bmatrix} \begin{Bmatrix} \hat{\boldsymbol{H}} \\ \hat{\boldsymbol{\Theta}} \end{Bmatrix} \tag{37}$$

Therefore, the impedance matrix in Eq. (2) can be finally obtained as

$$[\mathfrak{R}] = \begin{bmatrix} \Delta \boldsymbol{X} & \boldsymbol{0} \\ \boldsymbol{0} & \Delta \boldsymbol{Y} \end{bmatrix}^T \begin{bmatrix} \boldsymbol{A} & \boldsymbol{B} \\ \boldsymbol{C} & \boldsymbol{D} \end{bmatrix}^T \begin{bmatrix} \boldsymbol{X} & \boldsymbol{0} \\ \boldsymbol{0} & \boldsymbol{Y} \end{bmatrix} \tag{38}$$

The components in the impedance matrix are frequency-dependence and complex. The real part represents the springs which account for the effect of the restraining action of the supporting soil medium, whereas the imaginary part represents the dashpots which account for the effect of energy dissipation by radiation.

5. Impedance represented in time domain

The general form of each components $\mathfrak{R}_{ij}(\omega)$ in the impedance matrix $[\mathfrak{R}]$ can be normalized with respect to its corresponding static stiffness K_{ij}^s as $\mathfrak{R}_{ij}(a_0) = K_{ij}^s \overline{\mathfrak{R}}_{ij}(a_0)$. i, j=1, … , 2N, and $a_0=\omega L/(2V_s)$ is a dimensionless frequency. In order to perform the linear/nonlinear dynamic of structures including SSSI effect by the substructure method in time domain, a domain-transformation method has to be introduced to deal with those frequency-dependent impedances.

5.1. Impedance approximated by complex Chebyshev polynomial fraction

As suggested by Wolf [31], each component in impedance matrix can be treated separately by a lumped-parameter model, the subscripts i and j are omitted for simplicity, e.g. $\mathfrak{R}(a_0) = K^s \overline{\mathfrak{R}}(a_0)$. The normalized impedance $\overline{\mathfrak{R}}(a_0)$ is decomposed into a singular part which is equal to its asymptotic value $k^\infty + \mathrm{i}a_0 c^\infty$ for $a_0 \to \infty$, and a regular part which is represented as a ratio of two polynomials. Generally, a more complex impedance would have required a polynomial of higher order. As discussed later, actual impedances including cross-interference often show strong frequency dependence. Therefore, to reduce the problem of wiggling of approximation by simple polynomials of higher degree, the complex Chebyshev polynomials (the first eight terms as shown in Table 2) are introduced to enhance stability in numerical computation.

$$\bar{\Re}(a_0) \approx \tilde{\Re}(\mathrm{i}a_0) = k^{\infty} + \mathrm{i}a_0 c^{\infty} + \frac{1-k^{\infty} + \gamma_1 \tilde{T}_1(\mathrm{i}a_0) + \gamma_2 \tilde{T}_2(\mathrm{i}a_0) + \cdots + \gamma_M \tilde{T}_M(\mathrm{i}a_0)}{1+\chi + \mu_1 \tilde{T}_1(\mathrm{i}a_0) + \mu_2 \tilde{T}_2(\mathrm{i}a_0) + \cdots + \mu_{M+1} \tilde{T}_{M+1}(\mathrm{i}a_0)} \tag{39}$$

where χ in Eq. (39) has to be selected such that the doubly asymptotic feature $\bar{\Re}(a_0)$ can be ensured, i.e,

(i) It is exact in the static limit, $\bar{\Re}(a_0) \to 1$ for $a_0 \to 0$.

(ii) It is exact in the high-frequency limit, $\bar{\Re}(a_0) \to k^{\infty} + \mathrm{i}a_0 c^{\infty}$ for $a_0 \to \infty$.

Hence, we have

$$\chi = \begin{cases} \dfrac{1}{1-k^{\infty}} \displaystyle\sum_{m=1}^{M/2} (-1)^m \gamma_{2m} - \sum_{m=1}^{M/2} (-1)^m \mu_{2m} & M = 2,4,6\cdots \\ \dfrac{1}{1-k^{\infty}} \displaystyle\sum_{m=1}^{(M-1)/2} (-1)^m \gamma_{2m} - \sum_{m=1}^{(M-1)/2} (-1)^{m+1} \mu_{2m} + (-1)^{\frac{M-1}{2}} \mu_{M+1} & M = 1,3,5\cdots \end{cases} \tag{40}$$

The coefficients of the complex Chebyshev polynomials γ_s and μ_s can be obtained in an optimal manner based on the least squares fit. For any given foundation impedance, the values of these parameters can be uniquely determined. Reorganizing Eq. (39) gives the following complex polynomial fraction:

$$\tilde{\Re}(\mathrm{i}a_0) = k^{\infty} + \mathrm{i}a_0 c^{\infty} + \frac{1-k^{\infty} + a_1(\mathrm{i}a_0) + a_2(\mathrm{i}a_0)^2 + \cdots + a_M(\mathrm{i}a_0)^M}{1 + b_1(\mathrm{i}a_0) + b_2(\mathrm{i}a_0)^2 + \cdots + b_{M+1}(\mathrm{i}a_0)^{M+1}} \tag{41}$$

5.2. Lumped-parameter model

The polynomial fraction in Eq. (41) can be decomposed into a partial-fractions

$$\tilde{\Re}(\mathrm{i}a_0) = k^{\infty} + \mathrm{i}a_0 c^{\infty} + \sum_{m=1}^{2Y} \frac{X_m^*}{\mathrm{i}a_0 - t_m^*} + \sum_{m=Y+1}^{M-2Y} \frac{X_m}{\mathrm{i}a_0 - t_m} \tag{42}$$

where t_m and t_m^* are the real and complex roots of the denominator polynomial in Eq. (41), respectively. For a polynomial fraction with real coefficients, the real poles are associated with real residues X_m, whereas the complex poles would appear in complex conjugate pairs and their corresponding residues X_m^* are also in the form of complex conjugate pairs. Two conjugate first –order terms can be combined to a second-order term with real coefficients. Therefore, with *Y* pairs of complex conjugate poles among a total of *M* poles, Eq. (42) can be rewritten as

$$\tilde{\Re}(\mathrm{i}a_0) = k^{\infty} + \mathrm{i}a_0 c^{\infty} + \sum_{m=1}^{Y} \frac{\mathrm{i}a_0 \beta_m^{(1)} + \beta_m^{(2)}}{(\mathrm{i}a_0)^2 + \mathrm{i}a_0 \alpha_m^{(1)} + \alpha_m^{(2)}} + \sum_{m=1}^{M-2Y} \frac{X_m}{\mathrm{i}a_0 - t_m} \tag{43}$$

As a result, the total approximation of the impedance $K^s \bar{\Re}(a_0)$ consists of three characteristic types

(i) A singular term: $\left(k^{\infty} + \mathrm{i}a_0 c^{\infty}\right) K^s$ (44)

(ii) (*M*-*Y*) first-order term: $\left(\frac{X_m}{\mathrm{i}a_0 - t_m}\right) K^s$ (45)

(iii) *Y* second-order term: $\left(\frac{\mathrm{i}a_0 \beta_m^{(1)} + \beta_m^{(2)}}{(\mathrm{i}a_0)^2 + \mathrm{i}a_0 \alpha_m^{(1)} + \alpha_m^{(2)}}\right) K^s$ (46)

The above expressions can be interpreted as the frequency-response functions of the L-P models. In order to avoid the problem of modifying the driving loads or input motion at the nodes of the strip foundations, three discrete-element model with no mass was presented by Wolf [31] as shown in Fig. 3. The spring and damping coefficients in these models can be uniquely defined by the coefficients in Eqs. (44)-(46) as follows

$$\kappa = k^{\infty}, \quad \lambda = c^{\infty} \tag{47a}$$

$$\kappa_m = \frac{X_m}{t_m}, \quad \lambda_m = -\frac{X_m}{t_m^2} \tag{47b}$$

$$\kappa_m^{(1)} = -\frac{\beta_m^{(2)}}{\alpha_m^{(2)}}, \quad \lambda_m^{(1)} = \frac{\alpha_m^{(2)} \beta_m^{(1)} - \alpha_m^{(1)} \beta_m^{(2)}}{\left(\alpha_m^{(2)}\right)^2} \tag{47c}$$

$$\kappa_m^{(2)} = \frac{\beta_m^{(2)} \left(\alpha_m^{(1)} \beta_m^{(2)} - \alpha_m^{(2)} \beta_m^{(1)}\right)^2}{\left(\alpha_m^{(2)}\right)^2 \left[\alpha_m^{(2)} \left(\beta_m^{(1)}\right)^2 - \alpha_m^{(1)} \beta_m^{(1)} \beta_m^{(2)} + \left(\beta_m^{(2)}\right)^2\right]}, \quad \lambda_m^{(2)} = \frac{\left(\beta_m^{(2)}\right)^2 \left(\alpha_m^{(1)} \beta_m^{(2)} - \alpha_m^{(2)} \beta_m^{(1)}\right)}{\left(\alpha_m^{(2)}\right)^2 \left[\alpha_m^{(2)} \left(\beta_m^{(1)}\right)^2 - \alpha_m^{(1)} \beta_m^{(1)} \beta_m^{(2)} + \left(\beta_m^{(2)}\right)^2\right]} \tag{47d}$$

6. Convergence and validation

6.1. Convergence study

Convergence and numerical stability of the discretization method are investigated with respect to the number of segmental strip elements. The convergence characteristics in terms of segmental subdivisions of lateral and rocking impedances of a single foundation for various excitation frequencies are given in Table 3. It can be seen from Table 3 that lateral impedances converge

slightly faster than the rocking impedances.

6.2. Comparison studies

The Lamb's problem of finding the displacement at an arbitrary point on the surface of a half-space medium due to a harmonic concentrated line force applied at the origin was studied by Hasegawa et al. [16] with the thin layered method (TLM). To validate the numerical calculation of the Green functions in Eqs. (11) and (19), which contain multi-value improper integrals, the results of the displacement responses of half-space subjected to a uniform force are compared to those given by TLM, as shown in Fig. 4. The soil parameters are: soil density ρ_s=2000kg/m^3, shear wave velocity V_s=500m/s, Poisson's ratio v=0.4. Furthermore, we take the interval of the uniform harmonic excitation d=0.5m, which is small enough as a distance between the observation location and the excitation location S=40m. The excitation frequency is non-dimensionlized which can be expressed as $a_0=\omega S/(2V_s)$. As it is shown in Fig. 4, the lateral and the vertical responses obtained are close to those from the TLM. However, there are some minor differences between the results from the two methods. The present solution is more accurate than the TLM solution since the TLM method has to use the artificial boundary.

Luco et al. [10] presented the impedance of a massless rigid strip foundation intimately bonded to an elastic half-space by means of a rigorous analytical method. As the resulting integral equations presented considerable difficulties from the numerical point of view, only a special case for Poisson's ratio v=0.5 was solved in detail. The cases with Poisson's ratio v<0.5, valid for low frequencies $a_0\leq$1.5, were computed approximately using the dominant part of the singular integral equations. The lateral/rocking flexibilities of the foundation $\boldsymbol{F}=\mathfrak{R}^{-1}$ with respect to the dimensionless exciting frequency are compared with those given by the analytical method as shown in Figs. 5 and 6. It should be noted from Figs. 5 and 6 that the present method shows a consistency with the rigorous analytical method. In addition, the extended solutions in Fig. 6 further validate the results for higher frequencies.

7. Parameter studies to reveal cross-interference

7.1 Distribution of contact stress

The dynamic contact stresses of identical strip foundations in group are compared to those of a single one to reveal the significance of cross-interference. In this example, the contact stress distributions of a group of two foundations are shown in Figs. 7 and 8 and those of a group of three foundations are shown in Figs. 9 and 10. The distance ratio S/L=0.25, the Poisson's ratio ν=1/3, and different dimensionless frequencies a_0=0.5, 5 for the lateral-rocking harmonic excitations Q_0 and M_0. We define $\bar{x}$ as the local coordinate with the origin at the center of each foundation. The non-dimensional contact stresses are normalized as $\bar{q}=Lq/(Q_0)$, $\bar{p}=L^2p/(M_0)$. It can be seen from Figs. 7(a) and 8(a) that the stress distributions of a single foundation at a low frequency a_0=0.5 is similar to the static rigid distributions assumed by Sung [8]. However, there is a significant change for the case of a high frequency a_0=5.0 as shown Figs. 7(b) and 8(b). This indicates that the shape and magnitude of the contact stresses are quite sensitive to the variation of the vibration frequency.

Figs. 7-10 depict the influence of cross-interference on the distribution of dynamic contact stress. Unlike a single foundation of a symmetrical distribution of traction q and an anti-symmetrical distribution of traction p, a group of two foundations present skewed distributions of contact stresses as shown in Figs. 7 and 8. While the outside edges of the two foundations are still follow the distribution of a single foundation, there are deviations on the inside edges due to the influence from the adjacent foundation. For the case of three foundations in expected Figs. 9 and 10, the two side foundations in the group have similar distributions. The middle foundation has a symmetrical distribution of q and an anti-symmetrical distribution of p but their shapes and magnitudes are significantly different from those of a single one. Moreover, the stress distributions at the edges of adjacent foundations are quite close. Therefore, we can conclude that the assumption made on contact stress distributions such as the static rigid distribution which was commonly used will result in a considerable error in a SSSI analysis.

7.2 Influence of the distance ratio on impedance

Two identical strip foundations subjected to harmonic lateral/rocking excitations are used to investigate the influence of the ratio between separation distance to foundation width S/L on cross-interference. The variations of lateral and rocking impedances of a foundation with respect to different distance ratios (S/L=0.125, 0.5, 3, 5, 10, ∞) are displayed in Figs. 11 and 12. It can be seen

that the lateral and rocking impedances of two foundations in the case of closely spaced distance ratio such as S/L=0.125 fluctuate around that of a single foundation. In general, the cross-interference would make the impedances more frequency dependent. Moreover, the influence from the adjacent foundation is not significant in the case of large distance ratio such as S/L=5.0.

7.3 Impedance for a group of three strip foundations

The lateral-rocking vibrations of a group of three identical strip foundations equidistantly spaced at a distance ratio S/L=0.5 on an elastic half-space with Poisson's ratio v=1/3 are studied. The lateral and rocking impedances of each foundation due to cross-interference are presented and compared to the results of a single foundation, as shown in Figs. 13 and 14, in which the coefficients K_{ii} and C_{ii} (i=1,2,3) are referred to the normalized self-correlative stiffness and damping of the foundations in the group, while K_{ij} and C_{ij} ($i \neq j$, i,j=1,2,3) are referred to the normalized cross-correlative stiffness and damping between foundation i and foundation j. The coefficients K_{sig} and C_{sig} are those without the consideration of the cross-interference effect among foundations. It can be seen from Figs. 13 and 14 that the impedances of each foundation fluctuate around that of a single foundation. It is also observed that the middle foundation experiences a greater cross-interference effect compared to those on the side. Once again it is confirmed that the distance ratio S/L is an important factor as far as cross-interference is concerned.

8. Lumped-parameter model for adjacent foundations

This example seeks to establish an L-P model to simulate adjacent foundations on a homogeneous elastic half-space. Consider two strip foundations of different width $2m$ and $4m$, separated by a distance of $2m$. The soil parameters are: density ρ_s=2000kg/m^3, shear wave velocity V_s=200m/s, Poisson's ratio v=0.3. The normalized impedances in frequency domain, which are based on the discretization method presented in this paper, are used to curve-fit the L-P model. The optimal coefficients of polynomial-fraction fitted by different numbers of terms of complex Chebyshev polynomials are listed in Table 4. The simulated impedances in time domain are depicted in Figs. 15-17. It can be seen from Figs. 15-17 that results are highly consistent between the solutions of L-P models in time domain and those of the discretization method in frequency domain. The L-P model

gives promising simulations to $\mathfrak{R}_{aa}^{hh}$, $\mathfrak{R}_{aa}^{rr}$, $\mathfrak{R}_{bb}^{hh}$, $\mathfrak{R}_{bb}^{hh}$, and $\mathfrak{R}_{ab}^{hh}$ when the order of the complex Chebyshev polynomial increases up to M=6. The L-P model gives satisfactory simulation to $\mathfrak{R}_{ab}^{rr}$ when the order of the complex Chebyshev polynomial increases up to M=5. With the optimal parameters determined by the L-P model, normalized stiffness and damping coefficients are plotted in Fig. 18. This model can be incorporated with the substructure method for SSSI analysis in time domain, in which the superstructures can even be non-linear.

9. Conclusions

A systematic procedure has been presented in this paper for the solution of a SSSI problem based on the substructure approach. The discretization method is presented to determine the contact stress distribution and impedance matrix of the lateral/rocking dynamic of a surface strip foundation group. With a clear physical interpretation, the model can be easily adopted by engineers for dynamic analysis and seismic design of closely spaced strip foundations. After some parametric studies of cross-interference effect, following conclusions can be drawn:

(1) The discretization method avoids directly solving the contact stress functions at soil-foundation interfaces which, in general, cannot be expressed by elementary functions. Unlike the mixed boundary-value method, which requires solutions of dual integral equations in terms of elementary functions even for a single foundation, the proposed method based on a discretization can be applied directly to multiple foundations. The accuracy and the validity over a wide frequency range have been verified by the convergence studies and the comparison with existing results.

(2) The distributions of dynamic contact stress are sensitive to the frequency of excitation. Due to the influence of the cross-interference, adjacent foundations present skewed distributions of the contact stress. As a result, a considerable error would be introduced, if the SSSI problem is analyzed by a stress boundary-value method based on a stress distribution assumption.

(3) The distance ratio S/L greatly influences the dynamic cross-interaction, especially for a small ratio less than 5.0. As for foundations located in different positions of the group, the center

foundation generally suffers a greater SSSI effect than the side ones. The impedance of strip foundations in a group shows a stronger frequency-dependent characteristic than that of a single one.

Finally, an L-P model based on complex Chebyshev polynomial fraction is proposed to determine the frequency-dependent impedances in a time domain for the linear/nonlinear dynamic analysis of structure-soil-structure interaction by means of a substructure method.

Acknowledgements

The financial supports from the HKSAR GRF Grant (HKU 71511OE) and the Natural Science Foundation of Jiangsu Province, China (SBK201322459) are greatly acknowledged.

References

[1] E. Kausel, Early history of soil–structure interaction, Soil Dyn. Earthq. Eng. 30(9) (2010) 822-832.

[2] H. Mizuno, Effects of structure-soil-structure interaction during various excitations, in: Proceedings of the 7th World Conference on Earthquake Engineering, Isanbul, Turkey, 1980, pp: 149-156.

[3] Y. Kitada, T. Hirotani, M. Iguchi, Models test on dynamic structure–structure interaction of nuclear power plant buildings, Nucl. Eng. Des. 192(2) (1999) 205-216.

[4] T. Chrysoula, W. Armand, Simulation of seismic response in an idealized city, Soil Dyn. Earthq. Eng. 23(5) (2003) 391-402.

[5] M. Yahyai, M. Mirtaheri, M. Mahoutian, A. Daryan, Soil structure interaction between two adjacent buildings under earthquake load, Am. J. Eng. Appl. Sci. 1(2) (2008) 121-125.

[6] S. Kocak, Y. Mengi, A simple soil–structure interaction model, Appl. Math. Model. 24 (2000) 607-635.

[7] E. Reissner, Stationare axialsymmetrische durch eine sehuttelnde masseerregte sehwingungen eines homogenen elastisehen halbraumes, Ingenieur-Arch. 7(6) (1936) 381-396.

[8] T.Y. Sung, Vibration in semi-infinite solids due to periodic surface loadings, Symp. Dyn. Test Soil. 156(1) (1953) 35-64.

[9] I. Anam, J.M. Roësset, Dynamic stiffnesses of surface foundations: an explicit solution, Int. J. Geomech. 4(3) (2004) 216-223.

[10] J.E. Luco, R.A. Westmann, Dynamic response of a rigid footing bonded to an elastic half-space, J. Eng. Mech. Div. ASME. 39(2) (1972) 527-534.

[11] G.R. Wickham, The forced two dimensional oscillations of a rigid strip in smooth contact with a semi-infinite elastic solid, Math. Proc. Cambridge. 81(1977) 291-311.

[12] Y.Q. Cai, Y.M. Cheng, S.K. Au, C.J. Xu, X.H. Ma, Vertical vibration of an elastic strip footing on saturated soil, Int. J. Numer. Anal. Meth. Geomech. 32(5) (2008) 493-508.

[13] X.H. Ma, Y.M. Cheng, S.K. Au, Y.Q. Cai, C.J. Xu, Rocking vibration of a rigid strip footing on saturated soil, Comput. Geotech. 36(6) (2009) 928-933.

[14] G.B. Warburton, J.D. Richardson, J.J. Webster. Forced vibrations of two masses on an elastic half space, J. Appl. Mech., ASME, 38 (1971) 148-156.

[15] Z. Hryniewicz, Dynamic response of a rigid strip on an elastic half-space, Comput. Meth. Appl. Mech.

Eng. 25(3) (1981) 355-364.

[16] M. Hasegawa, S. Nakai, N. Fukuwa, An application of two-dimensional point load solutions by the thin layered method: Part I derivation of point load solution, AIJ. 58(1983) 785-786(in Japanese).

[17] T. Jiang, X.X. Song, Analysis of impedance functions of strip foundations embedded in stratified soils by using thin layer method, Chinese Quart Mech. 30(1) (2009) 62-70(in Chinese).

[18] J. Wang, D. Zhou, W.Q. Liu, S.G. Wang, Rocking response of a surface-supported strip foundation under a harmonic swaying force, Appl. Mech. Mat. 226(2012) 1453-1457.

[19] J. Wang, D. Zhou, W.Q. Liu, S.G. Wang, D.S. Du, Impedance Function of a Surface-supported strip Foundation based on elastic half-space Green functions, Chinese Quart Mech. 34(2) (2013) 262-269(in Chinese).

[20] G. Lin, Z. Han, H. Zhong, S.G. Wang, D.S. Du, A precise integration approach for dynamic impedance of rigid strip footing on arbitrary anisotropic layered half-space, Soil Dyn. Earthq. Eng. 49(1) (2013) 96-108.

[21] H.L. Wong, J.E. Luco, Dynamic interaction between rigid foundations in a layered half space, Soil Dyn. Earthq. Eng., 5 (1986) 149-158.

[22] S.A. Savidis, T. Richter, Dynamic interaction of rigid foundations, in: Proceedings of the 9th International Conference on Soil Mechanics and Foundation Engineering, Tokyo, Japan, 1977, pp: 369-374.

[23] S. Wang, G. Schmid, Dynamic structure-soil-structure interaction by FEM and BEM, Comput. Mech. 9(5) (1992) 347-357.

[24] H. Lamb, On the propagation over the surface of an elastic solid, Philos. Trans. R. Soc. A. 203(1) (1904) 1-42.

[25] P. Zheng, B. Ding, S.X. Zhao, D. Ding, 3D dynamic Green's functions in a multilayered poroelastic half-space, Appl. Math. Model. 37 (2013) 10203-10219.

[26] Y. Wang, R. Rajapakse, A.H. Shah, Dynamic interaction between flexible strip foundations, Earthq. Eng. Struct. Dyn. 20(5) (1991) 441-454.

[27] T. Senjuntichai, W. Kaewjuea, Dynamic response of multiple flexible strips on a multilayered poroelastic half-plane, J. Mech. Mat. Struct. 3(10) (2008) 1885-1901.

[28] J. Wang, D. Zhou, W.Q. Liu, Horizontal impedance of pile groups considering shear behavior of multilayered soils, Soils Found. 54(5) (2014) In press.

[29] J. Wang, S.H. Lo, D. Zhou, Effect of a forced harmonic vibration pile to its adjacent pile in layered elastic soil with double shear model, Soil Dyn. Earthq. Eng. (2015) In press.

[30] M. Saitoh, Simple model of frequency-dependent impedance functions in soil-structure interaction using frequency-independent elements, J. Eng. Mech. 133(10) (2007) 1101-1114.

[31] J.P. Wolf, Consistent lumped‐parameter models for unbounded soil: Physical representation, Earthq. Eng. Struct. Dyn. 20(1) (1991) 11-32.

[32] J.P. Wolf, Foundation vibration analysis using simple physical models, Prentice-Hall: Englewood Cliffs, NJ, 1994.

[33] J.P. Wolf, Spring‐dashpot‐mass models for foundation vibrations, Earthq. Eng. Struct. Dyn. 26(9) (1997) 931-949.

[34] E. Şafak, Time-domain representation of frequency-dependent foundation impedance functions, Soil Dyn. Earthq. Eng. 26(1) (2006) 65-70.

[35] W.H. Wu, W.H. Lee, Systematic lumped-parameter models for foundations based on polynomial‐fraction approximation, Earthq. Eng. Struct. Dyn. 31(7) (2002) 1383-1412.

[36] W.H. Wu, W.H. Lee, Nested lumped-parameter models for foundation vibrations, Earthq. Eng. Struct. Dyn. 33(9) (2004) 1051-1058.

[37] H. Wang, W.Q. Liu, D. Zhou, S.G. Wang, D.S. Du, Lumped-parameter model of foundations based on complex Chebyshev polynomial fraction, Soil Dyn. Earthq. Eng. 50(1) (2013) 192-203.

[38] L. Andersen, Assessment of lumped-parameter models for rigid footings, Comput. Struct. 88(23) (2010) 1333-1347.

[39] D. Zhou, Three-dimensional vibration analysis of structural elements using Chebyshev-Ritz method, Science Press, Beijing, China, 2007.

[40] A.H. Bhrawy, M.M. Tharwat, A. Yildirim. A new formula for fractional integrals of Chebyshev polynomials: Application for solving multi-term fractional differential equations, Appl. Math. Model. 37 (2013) 4245-4252.

Appendix

$\overline{A}_{mn}^{ij}$, $\overline{B}_{mn}^{ij}$ and $\overline{D}_{mn}^{ij}$ are multi-value improper integral, which can be valuated by the piecewise integration method.

$$\overline{A}_{mn}^{ij}=\frac{1}{\pi G_s}\left(f_{a1}+\mathrm{i}f_{a2}\right) \qquad \overline{B}_{mn}^{ij}=\frac{1}{\pi G_s}\left(f_{b1}+\mathrm{i}f_{b2}\right) \qquad \overline{D}_{mn}^{ij}=\frac{1}{\pi G_s}\left(f_{d1}+\mathrm{i}f_{d2}\right)$$

in which,

$$f_{a1}=-\frac{4V_s}{\omega}\int_{\vartheta}^{1}\frac{\eta^2\sqrt{\eta^2-\vartheta^2}(\eta^2-1)}{\left[(2\eta^2-1)^4-16\eta^4(\eta^2-\vartheta^2)(\eta^2-1)\right]\eta}G_1(\eta)d\eta-\overline{\mathrm{P}}\frac{V_s}{\omega}\int_{1}^{\infty}\frac{\sqrt{\eta^2-1}}{\left[(2\eta^2-1)^2-4\eta^2\sqrt{\eta^2-\vartheta^2}\sqrt{\eta^2-1}\right]\eta}G_1(\eta)d\eta$$

$$f_{a2}=-\frac{V_s}{\omega}\int_{0}^{\vartheta}\frac{\sqrt{1-\eta^2}}{\left[(2\eta^2-1)^2+4\eta^2\sqrt{\vartheta^2-\eta^2}\sqrt{1-\eta^2}\right]\eta}G_1(\eta)d\eta-\frac{V_s}{\omega}\int_{\vartheta}^{1}\frac{\sqrt{1-\eta^2}(2\eta^2-1)^2}{\left[(2\eta^2-1)^4-16\eta^4(\eta^2-\vartheta^2)(\eta^2-1)\right]\eta}G_1(\eta)d\eta$$
$$+\pi\times\frac{V_s\sqrt{\varepsilon^2-1}}{\left[F(\eta)\eta\right]'\big|_{\eta=\varepsilon}\omega}G_1(\varepsilon)$$

$$f_{b1}=-\frac{V_s}{\omega}\int_{0}^{\vartheta}\frac{2\eta^2-1+2\sqrt{1-\eta^2}\sqrt{\vartheta^2-\eta^2}}{(2\eta^2-1)^2+4\eta^2\sqrt{\vartheta^2-\eta^2}\sqrt{1-\eta^2}}G_2(\eta)d\eta-\frac{2V_s}{\omega}\int_{\vartheta}^{1}\frac{(4\vartheta^2-2)\eta^4+(3-4\vartheta^2)\eta^2-1}{(2\eta^2-1)^4-16\eta^4(\eta^2-\vartheta^2)(\eta^2-1)}G_2(\eta)d\eta-$$
$$\overline{\mathrm{P}}\frac{V_s}{\omega}\int_{1}^{\infty}\frac{2\eta^2-1-2\sqrt{\eta^2-1}\sqrt{\eta^2-\vartheta^2}}{(2\eta^2-1)^2-4\eta^2\sqrt{\eta^2-\vartheta^2}\sqrt{\eta^2-1}}G_2(\eta)d\eta$$

$$f_{b2}=-\frac{V_s}{\omega}\int_{\vartheta}^{1}\frac{(4\eta^2-2)\sqrt{\eta^2-\vartheta^2}\sqrt{1-\eta^2}}{(2\eta^2-1)^4-16\eta^4(\eta^2-\vartheta^2)(\eta^2-1)}G_2(\eta)d\eta+\pi\times\frac{\left(2\varepsilon^2-1-2\sqrt{\varepsilon^2-1}\sqrt{\varepsilon^2-\vartheta^2}\right)V_s}{\left[F(\eta)\right]'|_{\eta=\varepsilon}\,\omega}G_2(\varepsilon)$$

$$f_{d1}=-\frac{V_s}{\omega}\int_{\vartheta}^{1}\frac{\sqrt{\eta^2-\vartheta^2}(2\eta^2-1)^2}{\left[(2\eta^2-1)^4-16p^4(\eta^2-\vartheta^2)(\eta^2-1)\right]\eta}G_1(\eta)d\eta-\overline{\mathrm{P}}\frac{V_s}{\omega}\int_{1}^{\infty}\frac{\sqrt{p^2-\vartheta^2}}{\left[(2\eta^2-1)^2-4\eta^2\sqrt{\eta^2-\vartheta^2}\sqrt{\eta^2-1}\right]\eta}G_1(\eta)d\eta$$

$$f_{d2}=-\frac{V_s}{\omega}\int_{0}^{\vartheta}\frac{\sqrt{\vartheta^2-\eta^2}}{\left[(2\eta^2-1)^2+4\eta^2\sqrt{\vartheta^2-\eta^2}\sqrt{1-\eta^2}\right]\eta}G_1(\eta)d\eta-\frac{V_s}{\omega}\int_{\vartheta}^{1}\frac{4\eta^2(\eta^2-\vartheta^2)\sqrt{1-\eta^2}}{\left[(2\eta^2-1)^4-16\eta^4(\eta^2-\vartheta^2)(\eta^2-1)\right]\eta}G_1(\eta)d\eta$$
$$+\pi\times\frac{V_s\sqrt{\varepsilon^2-\vartheta^2}}{\omega\left[F(\eta)\eta\right]'|_{\eta=\varepsilon}}G_1(\varepsilon)$$

where ε is the root of $F(\eta)$, $\overline{\mathrm{P}}$ means the Cauchy principal value integral.

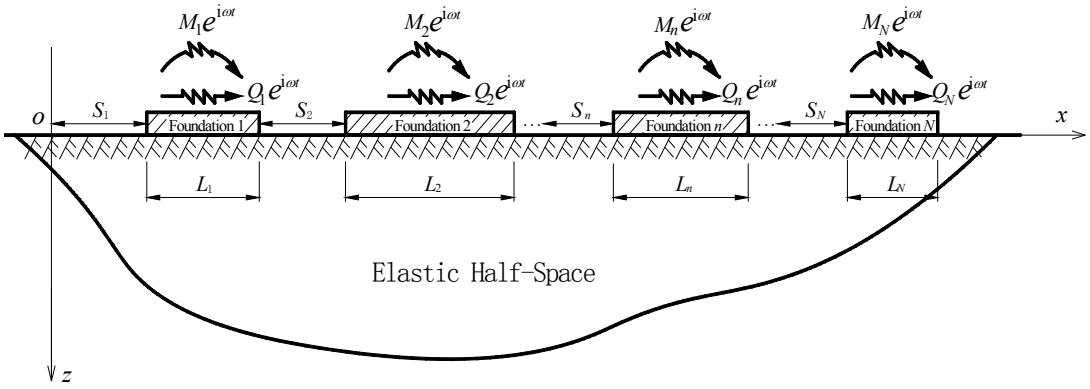

Fig. 1. The cross-sections of a group of long strip foundations attached to a semi-infinite soil medium under lateral/rocking harmonic excitations

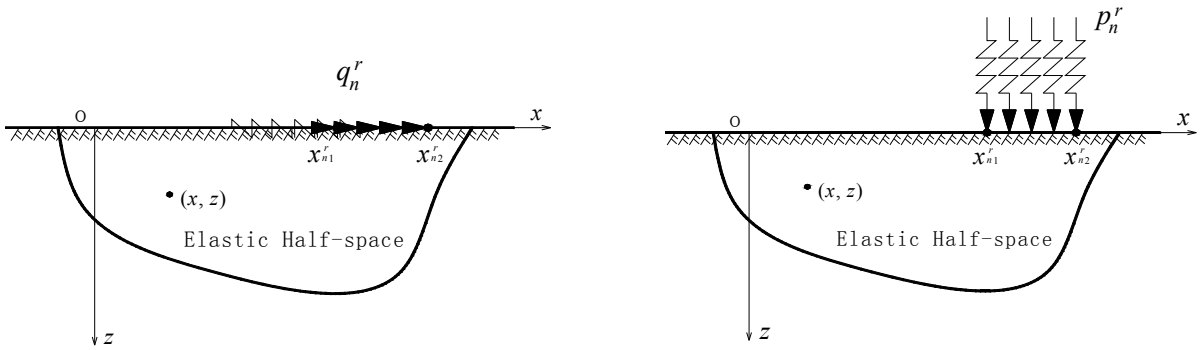

(a) (b)

Fig. 2. The half-space subject to a harmonic uniform load: (a) Lateral and (b) Vertical

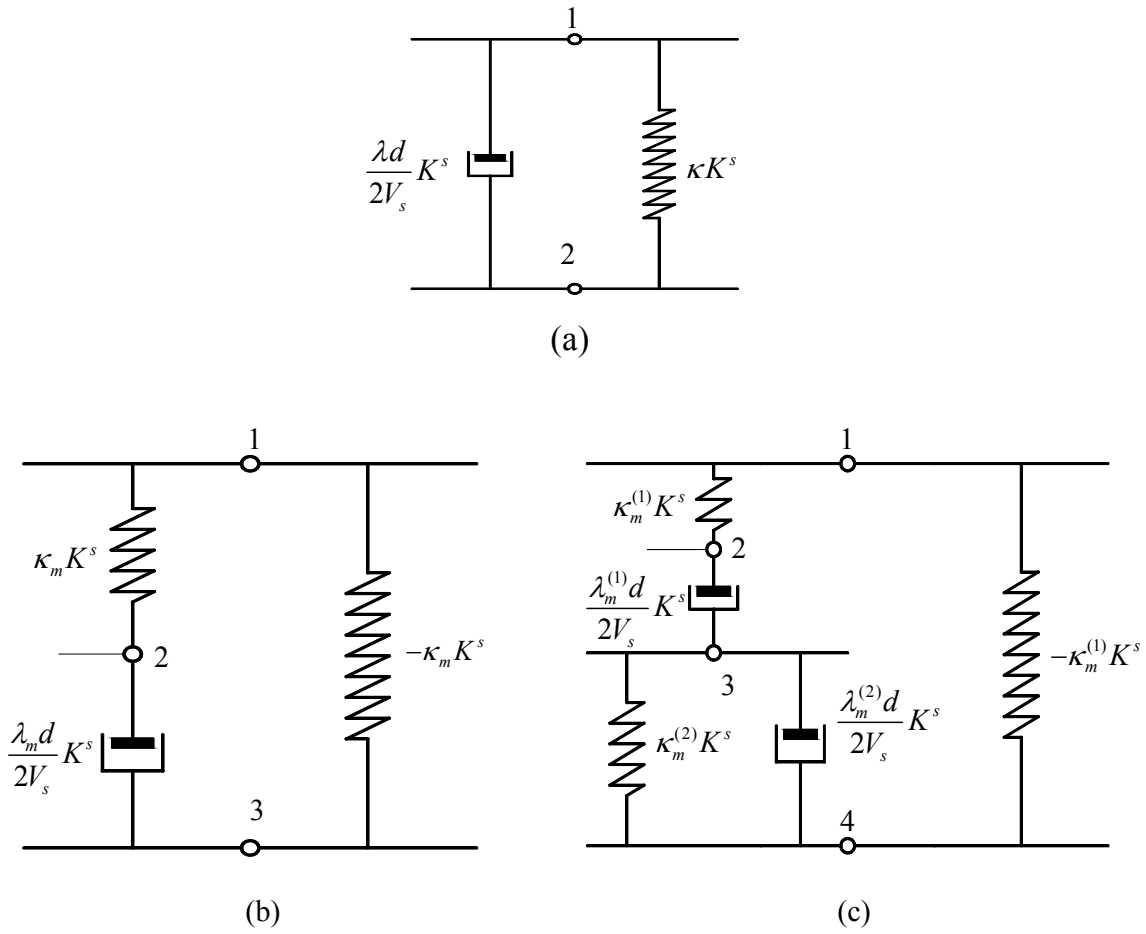

Fig. 3. Discrete-element models: (a) Singular term, (b) The first-order term and (c) The second-order term.

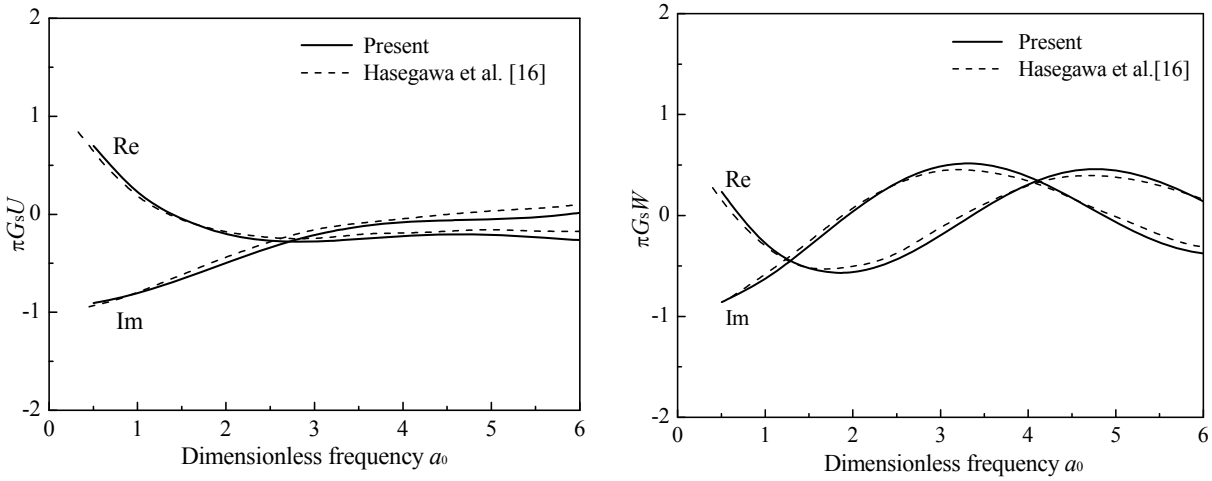

(a) (b)

Fig. 4. Displacement response of half-space under the harmonic excitation:

(a) lateral excitation and (b) vertical excitation

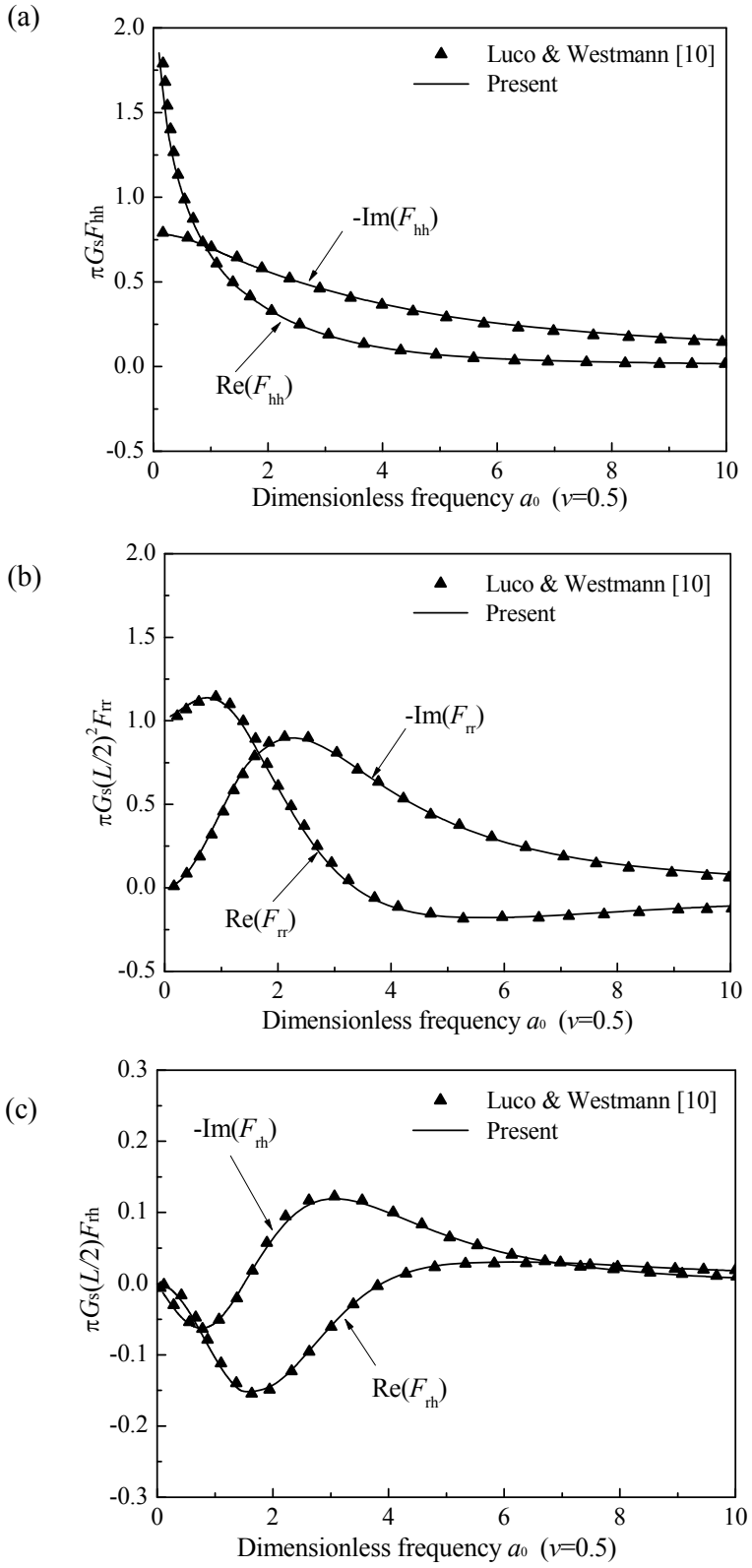

Fig. 5. Comparison of the present method with analytical solution:

(a) lateral, (b) rocking and (c) coupling

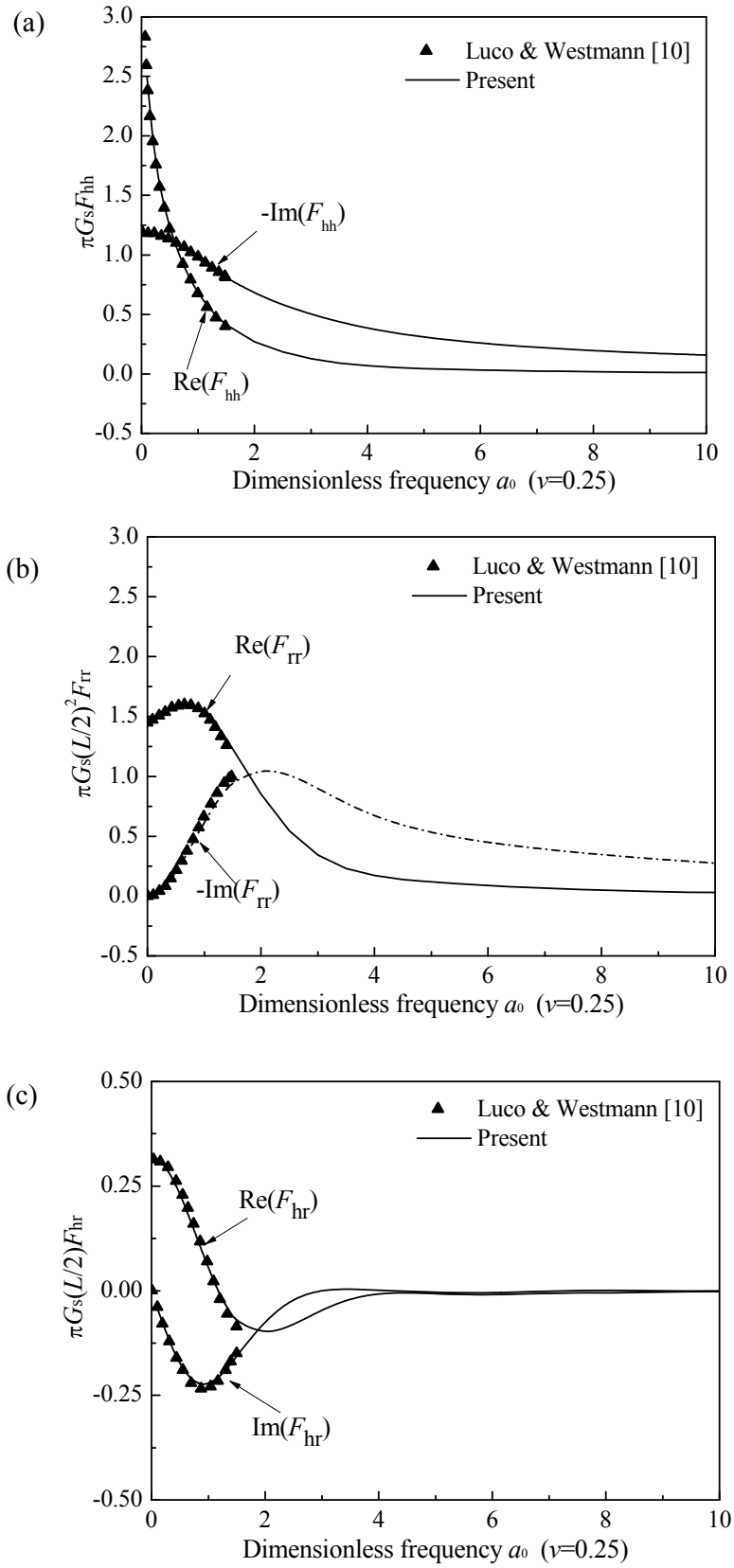

Fig. 6. Flexibility of a strip foundation for ν=0.25: (a) lateral, (b) rocking and (c) coupling

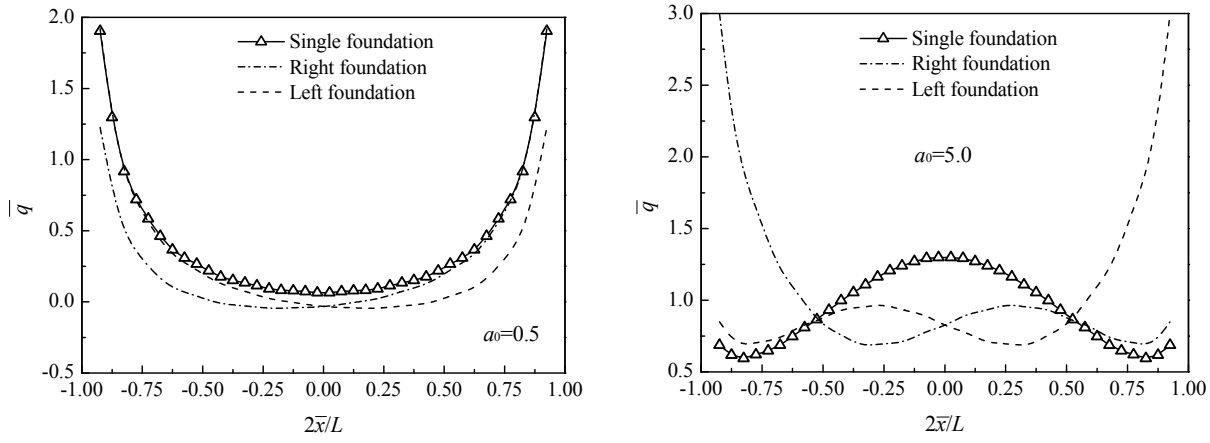

(a) a_0=0.5 (b) a_0=5.0

Fig. 7. The effect of cross-interference between two foundations on contact traction q

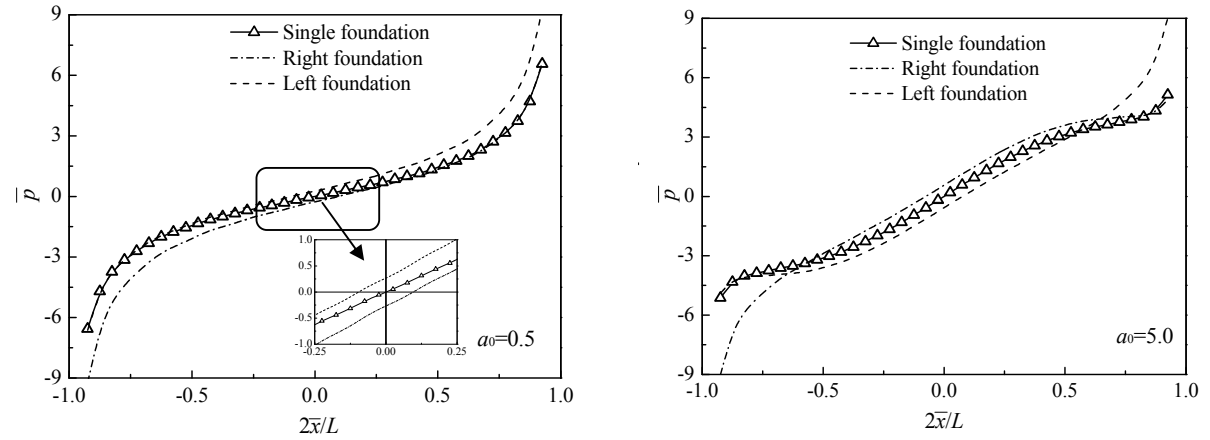

(a) a_0=0.5 (b) a_0=5.0

Fig. 8. The effect of cross-interference between two foundations on contact traction p

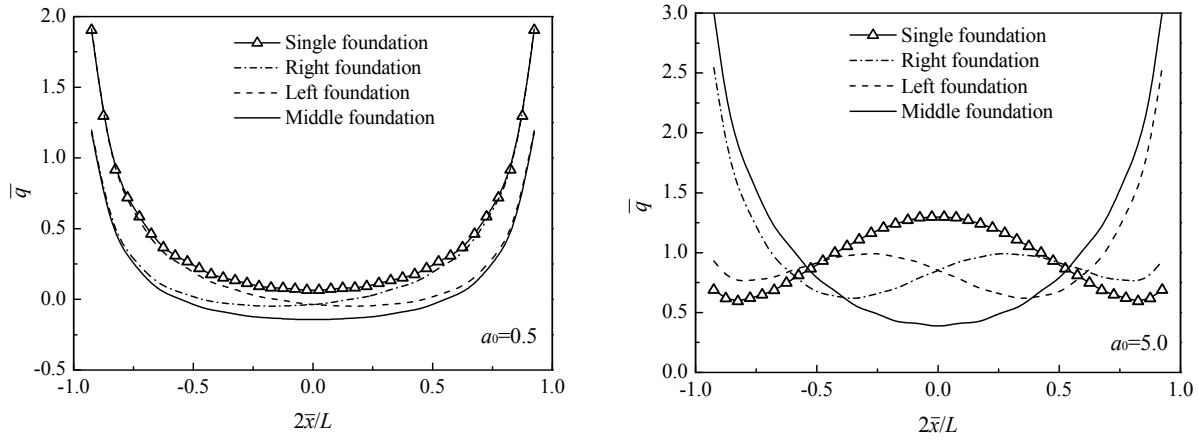

(a) a_0=0.5 (b) a_0=5.0

Fig. 9. The effect of cross-interference between three foundations on contact traction q

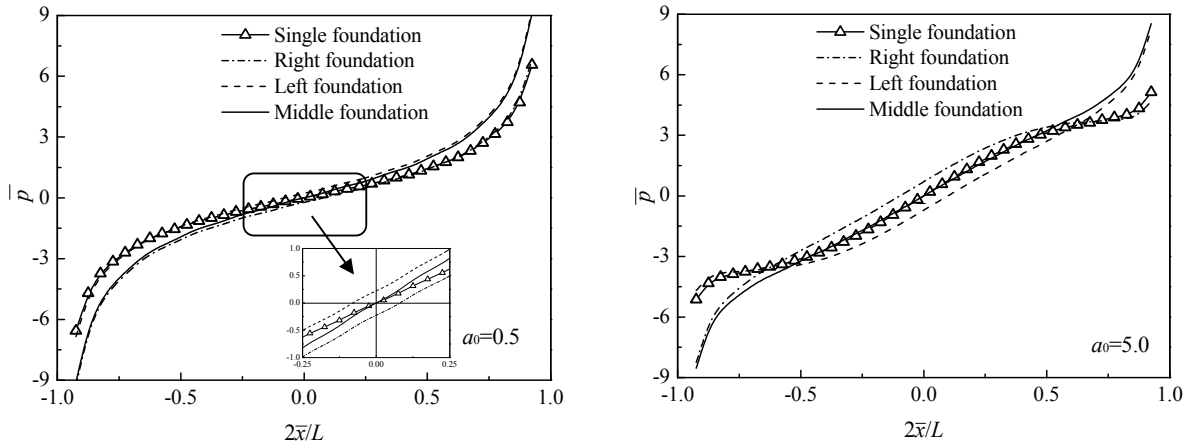

(a) a_0=0.5 (b) a_0=5.0

Fig. 10. The effect of cross-interference between three foundations on contact traction p

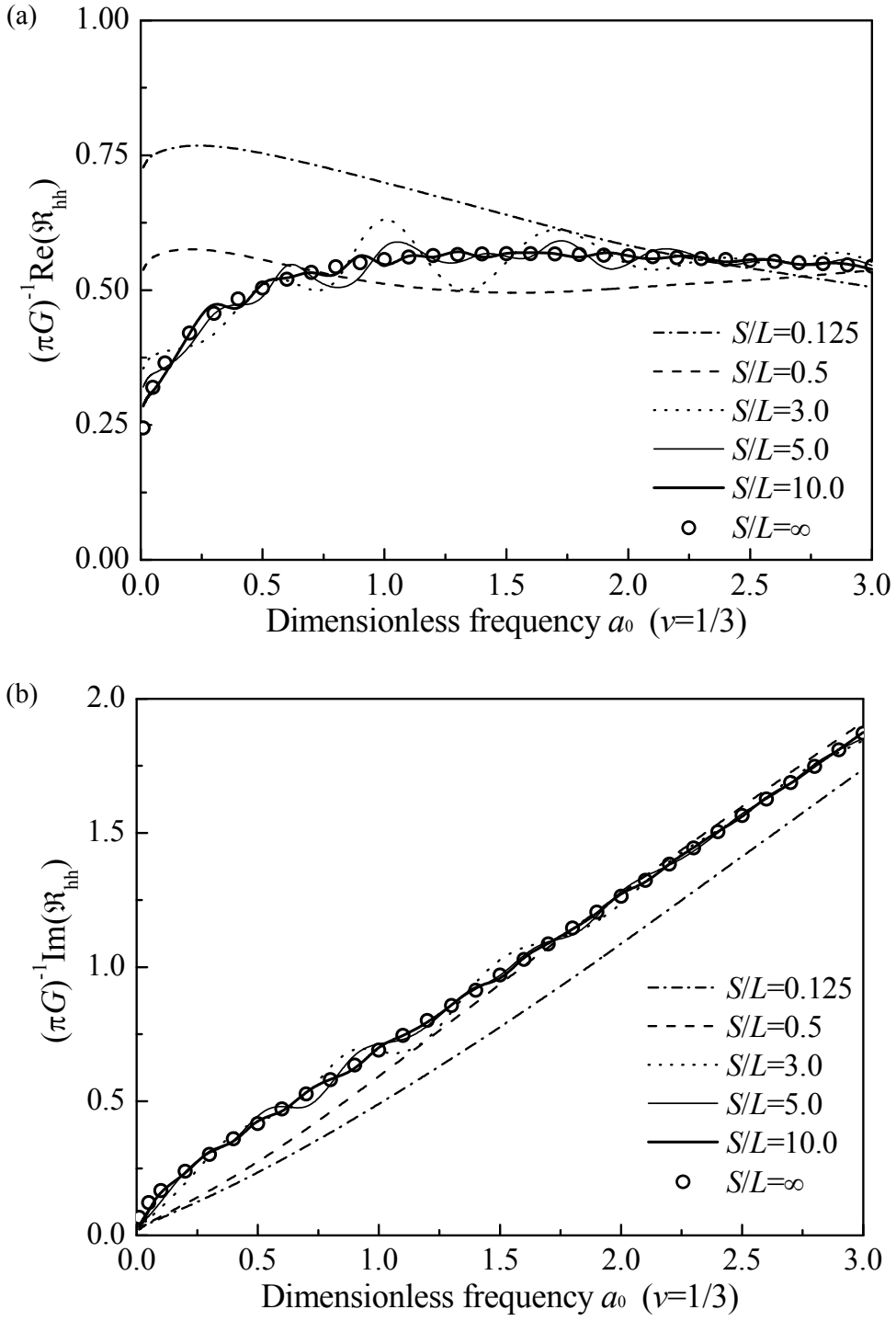

Fig. 11. Lateral impedance in consideration of cross-interference:

(a) Real part and (b) Imaginary part

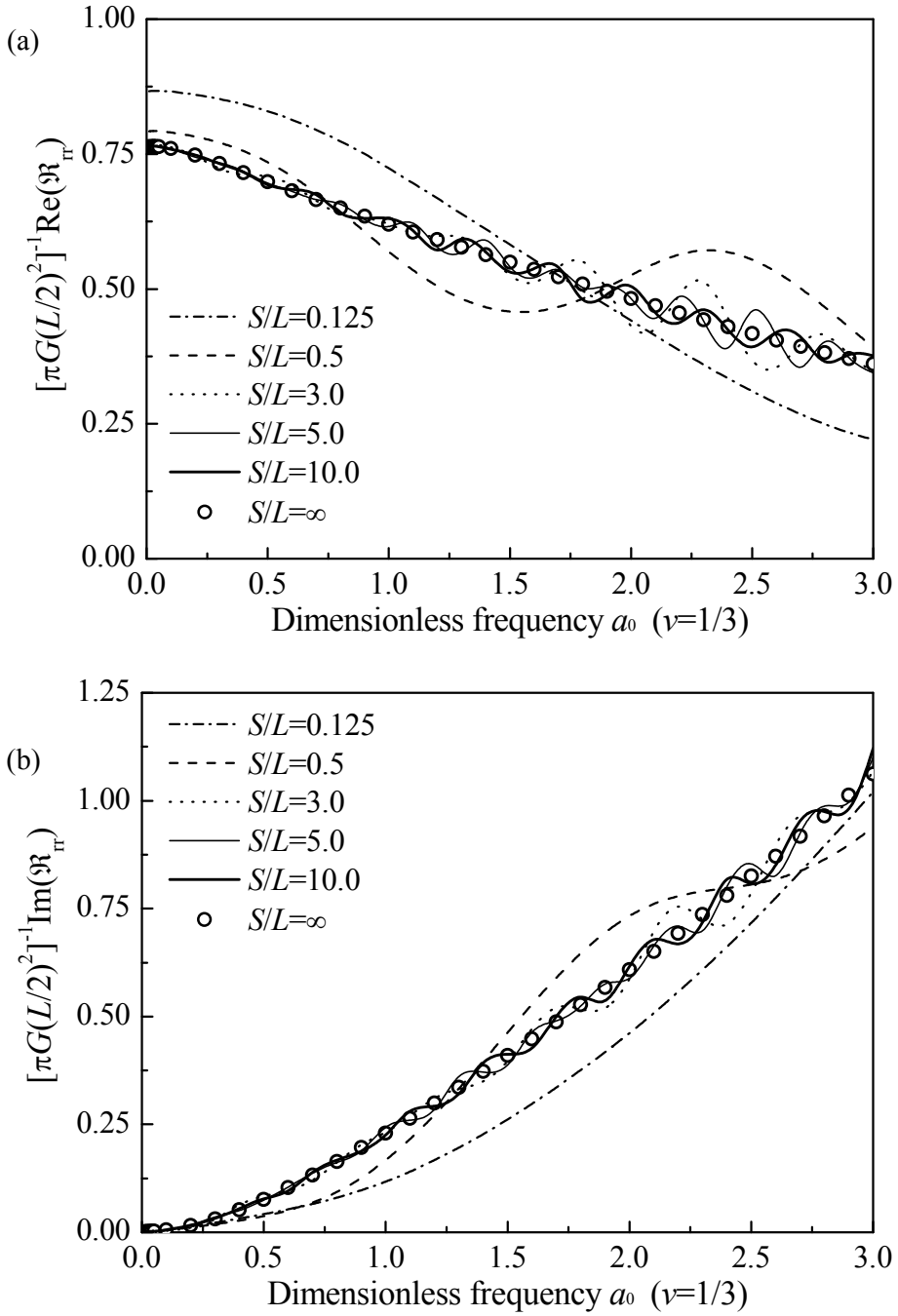

Fig. 12. Rocking impedance in consideration of cross-interference:

(a) Real part and (b) Imaginary part

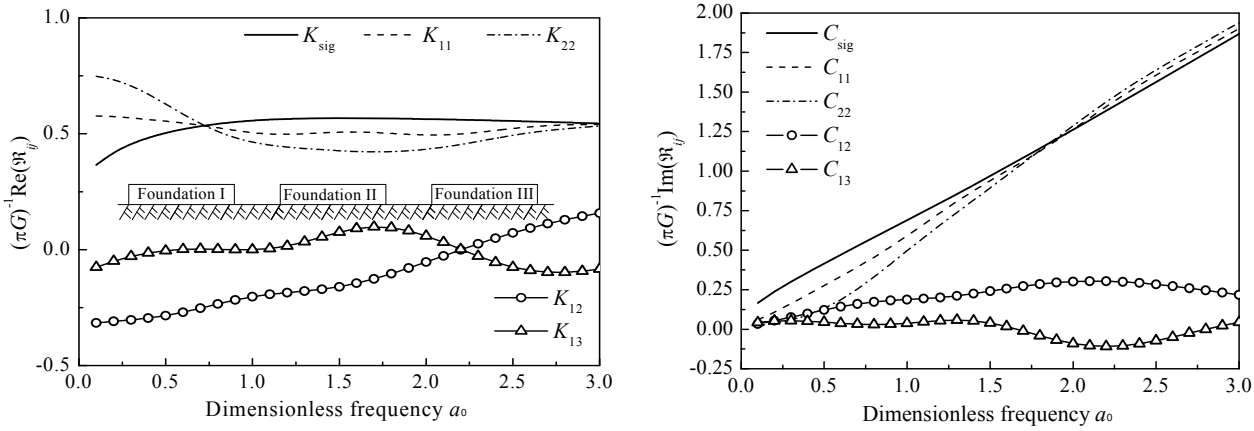

(a) (b)

Fig. 13. Lateral impedance of the strip foundation group: (a) Real part and (b) Imaginary part

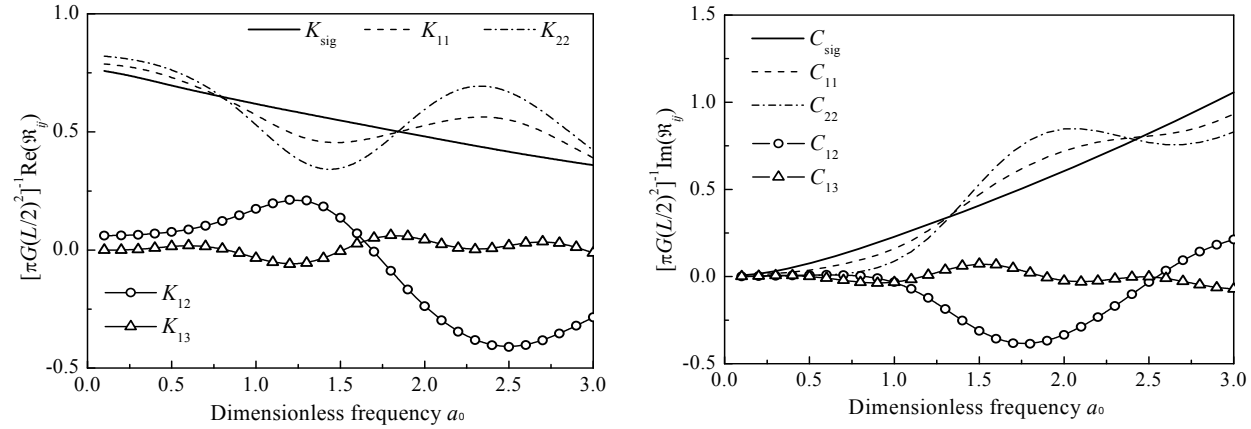

(a) (b)

Fig. 14. Rocking impedance of the strip foundation group: (a) Real part and (b) Imaginary part

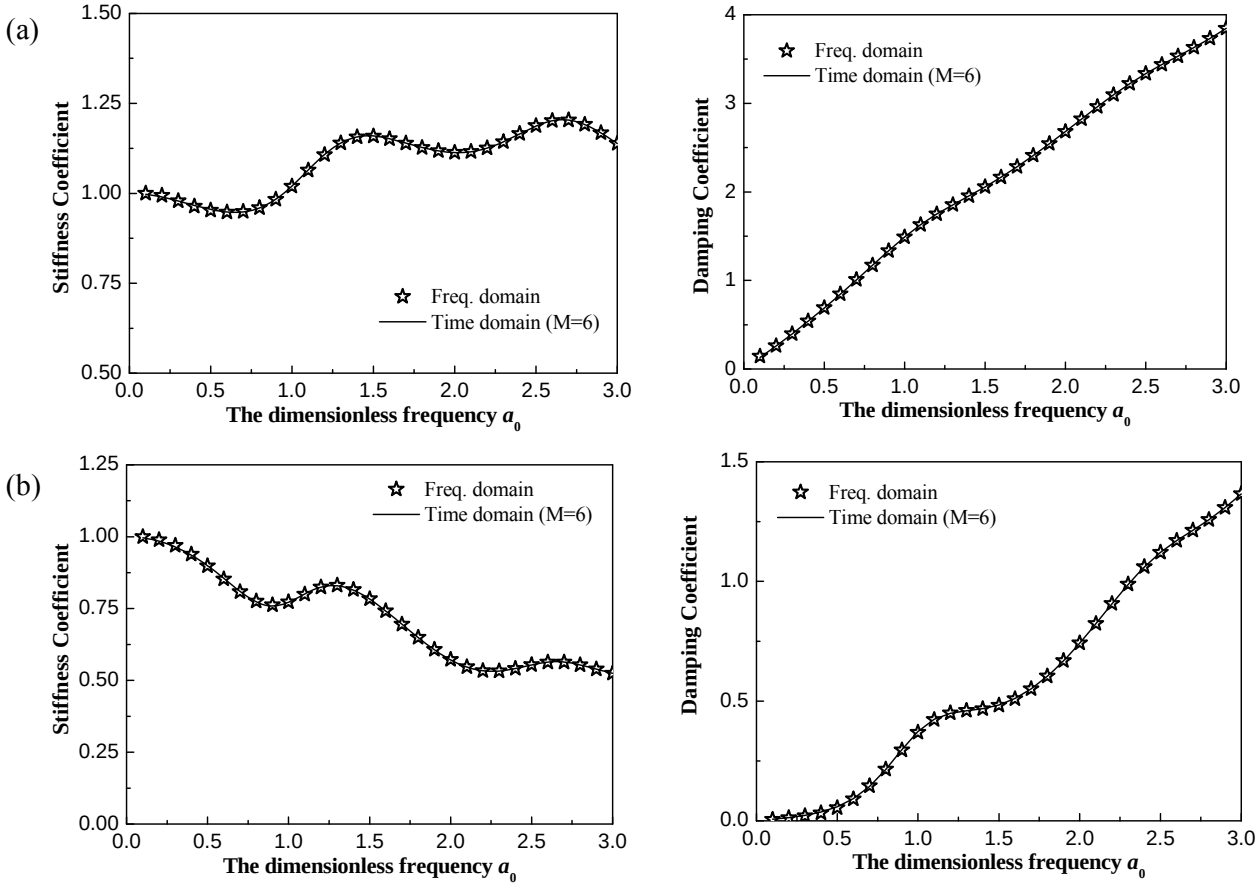

Fig. 15. Comparison of frequency and time domain impedances for Foundation I:

(a) Lateral impedance $\Re_{aa}^{hh}$ and (b) Rocking impedance $\Re_{aa}^{rr}$

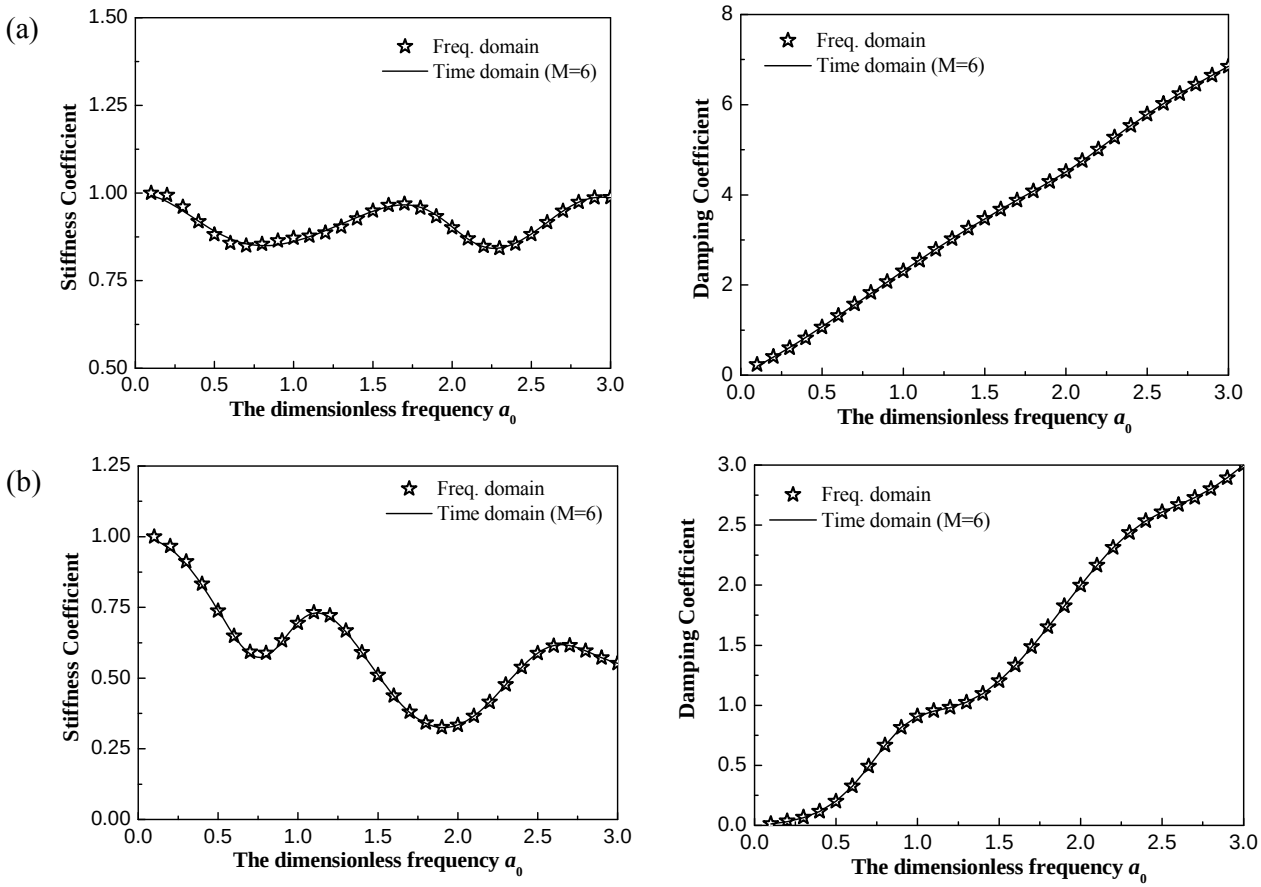

Fig. 16. Comparison of frequency and time domain impedances for Foundation II:

(a) Lateral impedance $\Re_{bb}^{hh}$ and (b) Rocking impedance $\Re_{bb}^{rr}$

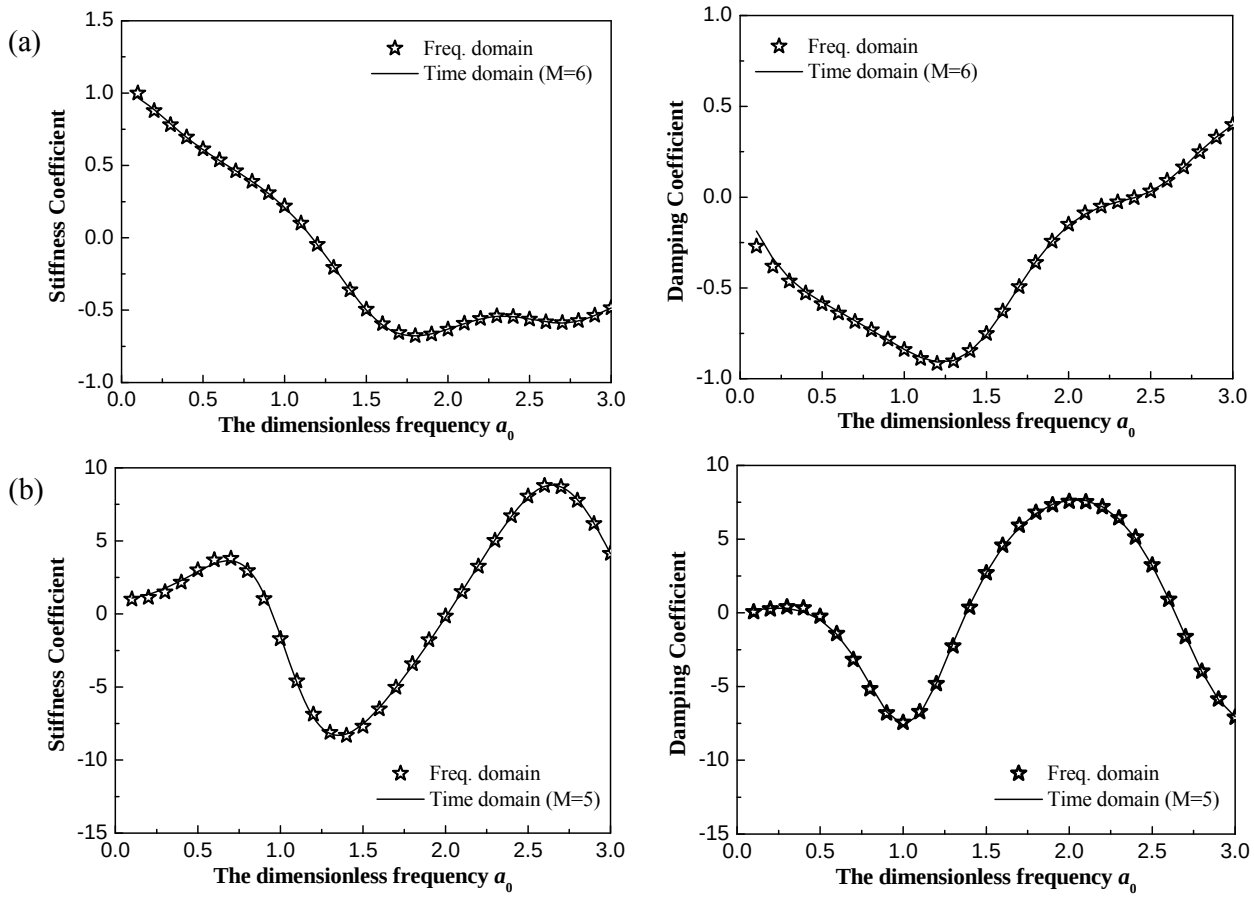

Fig. 17. Comparison of frequency and time domain coupling impedances for Foundation I and Foundation II: (a) Lateral impedance $\Re_{ab}^{hh}$ and (b) Rocking impedance $\Re_{ab}^{rr}$

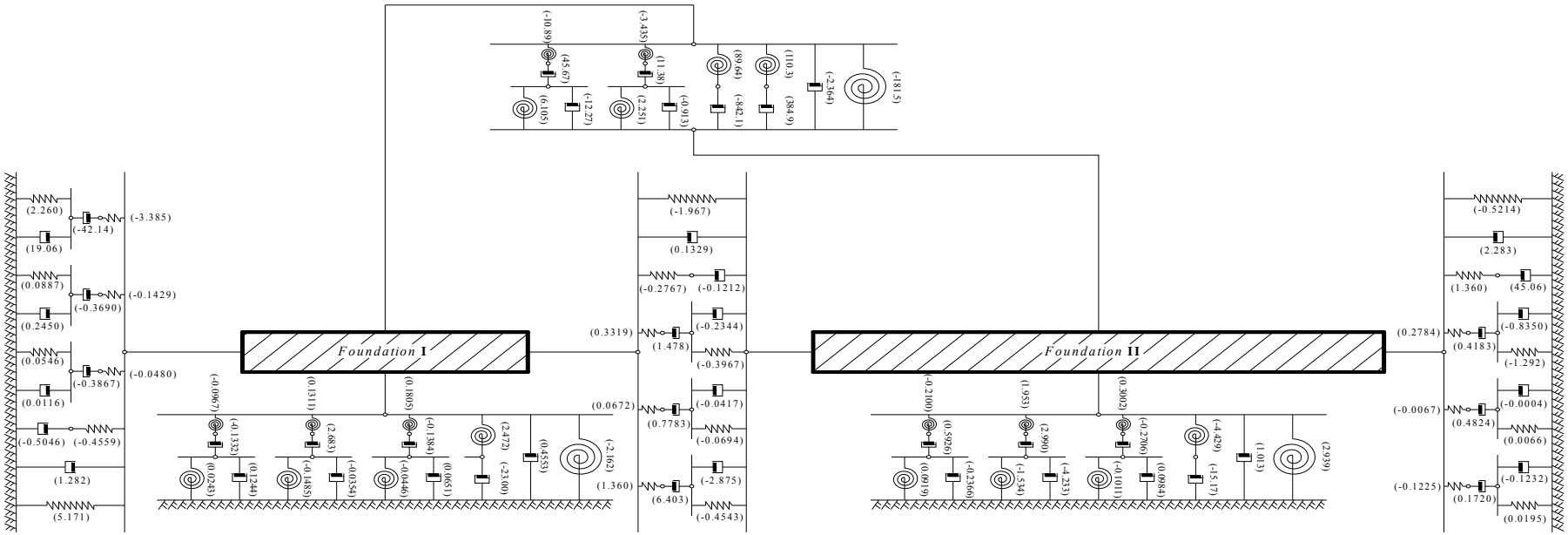

Fig. 18. Lumped-parameter model for the dynamic interaction of adjacent strip foundations

Table 1

Coordinate information of each element in the system

Coordinates	The r-th element in Footing 1 (r=1,…, R_1)	The r-th element in Footing n (r=1,…, R_n)	The r-th element in Footing N (r=1,…, R_N)
Central coordinate of each element	$C_1 = S_1 + \frac{(2r-1)L_1}{2R_1}$	$C_n = \frac{(2r-1)L_n}{2R_n} + \sum_{l=1}^{n}(S_l + L_{l-1})$	$C_N = \frac{(2r-1)L_N}{2R_N} + \sum_{l=1}^{N}(S_l + L_{l-1})$
Interval of each element	$\left[C_1 - \frac{\Delta_1}{2}, C_1 + \frac{\Delta_1}{2}\right]$	$\left[C_n - \frac{\Delta_n}{2}, C_n + \frac{\Delta_n}{2}\right]$	$\left[C_N - \frac{\Delta_N}{2}, C_N + \frac{\Delta_N}{2}\right]$

Table 2

The first eight complex Chebyshev polynomials $\tilde{T}_m(\tilde{x})$ (m=0, 1, 2, …,7)

$$\tilde{T}_0(\tilde{x}) = 1 = T_0(x)$$
$$\tilde{T}_1(\tilde{x}) = \tilde{x} = T_1(x)\mathrm{i}$$
$$\tilde{T}_2(\tilde{x}) = -2\tilde{x}^2 - 1 = T_2(x)$$
$$\tilde{T}_3(\tilde{x}) = -4\tilde{x}^3 - 3\tilde{x} = T_3(x)\mathrm{i}$$
$$\tilde{T}_4(\tilde{x}) = 8\tilde{x}^4 + 8\tilde{x}^2 + 1 = T_4(x)$$
$$\tilde{T}_5(\tilde{x}) = 16\tilde{x}^5 + 20\tilde{x}^3 + 5\tilde{x} = T_5(x)\mathrm{i}$$
$$\tilde{T}_6(\tilde{x}) = -32\tilde{x}^6 - 48\tilde{x}^4 - 18\tilde{x}^2 - 1 = T_6(x)$$
$$\tilde{T}_7(\tilde{x}) = -64\tilde{x}^7 - 112\tilde{x}^5 - 56\tilde{x}^3 - 7\tilde{x} = T_7(x)\mathrm{i}$$

Table 3

The convergence of the lateral/rocking impedance of a single strip foundation

N	a_0=0.25				a_0=2.0				a_0=3.0			
	Lateral		rocking		Lateral		Rocking		Lateral		Rocking	
	Re	Im	Re	Im	Re	Im	Re	Im	Re	Im	Re	Im
10	0.472	0.277	0.758	0.0220	0.623	1.25	0.470	0.603	0.618	1.84	0.291	1.04
20	0.274	0.280	0.787	0.0243	0.625	1.27	0.488	0.646	0.622	1.87	0.308	1.12
30	0.475	0.281	0.797	0.0245	0.626	1.28	0.493	0.660	0.622	1.88	0.312	1.14
40	0.475	0.281	0.801	0.0247	0.626	1.28	0.495	0.665	0.622	1.88	0.313	1.15
50	0.475	0.281	0.803	0.0248	0.626	1.29	0.496	0.669	0.622	1.88	0.314	1.16
60	0.475	0.282	0.806	0.0249	0.626	1.29	0.497	0.672	0.622	1.89	0.314	1.17
70	0.475	0.282	0.808	0.0250	0.626	1.29	0.498	0.675	0.622	1.89	0.315	1.17
80	0.475	0.282	0.809	0.0251	0.626	1.29	0.499	0.678	0.622	1.89	0.315	1.18
90	0.475	0.282	0.810	0.0251	0.626	1.29	0.500	0.679	0.622	1.89	0.315	1.18
100	0.475	0.282	0.810	0.0251	0.626	1.29	0.500	0.679	0.622	1.89	0.315	1.18

Note: Lateral impedances values above are normalized as $\Re_{hh}/(\pi G)$ and rocking impedances are normalized as $4\Re_{rr}/(\pi GL^2)$; the calculation parameters v=0.40, $a_0=\omega L/(2V_s)$

Table 4

The coefficients of the fitting polynomial fraction

	Foundation I		Foundation II		Coupling	
	Lateral	Rocking	Lateral	Rocking	Lateral	Rocking
	M=6	M=6	M=6	M=6	M=6	M=5
K^s	119261966	186979278	138714082	757741896	-70481684	17098126
k^∞	1.1385	0.5247	0.9877	0.5522	-0.4843	4.1436
c^∞	1.2821	0.4553	2.2832	1.0129	0.1329	-2.3640
a_1	1.7845	1.3599	2.2498	1.9045	2.8211	1.0314
a_2	1.6649	1.6973	2.1030	2.7042	1.7886	1.1811
a_3	1.0057	0.8522	1.1542	1.9747	1.3663	0.3742
a_4	0.2937	0.3797	0.5355	1.0380	0.2564	0.1044
a_5	0.0888	0.0650	0.1175	0.3461	0.1393	0.0114
a_6	0.0040	0.0134	0.0295	0.0826	-0.0014	-0.0030
a_7	0.0007	-0.0028	0.0008	0.0108	0.0042	-
b_1	-0.2401	0.2491	-0.2956	0.0101	2.1176	1.0796
b_2	0.0506	0.6529	-0.0433	0.6846	0.2111	-7.9259
b_3	-0.0640	0.0858	-0.1367	-0.1089	0.5335	5.0274
b_4	0.0589	0.1527	-0.0168	0.1640	-0.1082	-0.8401
b_5	-0.0041	0.0065	-0.0116	-0.0122	0.0331	0.5459
b_6	0.0057	0.0096	-0.0013	0.0104	-0.0126	-